Theory of second-harmonic generation from multilayer systems based on electric point-dipole radiation: Application to magnetic multilayers

Jaroslav Hamrle*
Laboratoire de Physique des Solides, UMR CNRS 8502, Bat. 510, Université Paris-Sud, 91405 Orsay, France and Institute of Physics, Charles University, Ke Karlovu 3, 121 16, Prague, Czech Republic

L'uboš Polerecký
Laboratoire de Physique des Solides, UMR CNRS 8502, Bat. 510, Université Paris-Sud, 91405 Orsay, France and Optical Sensors Laboratory, School of Physical Sciences, Dublin City University, Dublin 9, Ireland

Jacques Ferré
Laboratoire de Physique des Solides, UMR CNRS 8502, Bat. 510, Université Paris-Sud, 91405 Orsay, France
(Received 17 December 2002; revised manuscript received 10 June 2003; published 2 October 2003)

A complete and comprehensive theory of the propagation of second-harmonic (SH) field generated within arbitrary multilayer systems is presented. The theory is based on the radiation of point dipoles whose strength is determined by the distribution of the fundamental field interrogating the multilayer structure. The theory is applied to the study of magnetic-induced second-harmonic generation (MSHG) where the SH field is generated at the interfaces of the multilayer structure as a consequence of the local symmetry breaking, not only due to the structural asymmetry but also the local magnetization. In comparison with the already existing theory based on radiation of an infinitesimally thin polarization sheet, the approach based on the point-dipole radiation presented in this work is more general since it can be applied to the study of systems whose susceptibility tensors, which describe the nonlinear properties of the media, exhibit arbitrary spatial variations. It is shown that the Fourier transform of such variations is closely related to the angular variation of the observable intensity of the far-field SH. Due to the point-dipole nature of the approach used, the theory presented here can be employed in the analysis of MSHG from systems with (buried) magnetic domains with sizes comparable to the wavelength of the second harmonic light, magnetic nanostructures, and others. In addition to the formalism itself, a number of numerical examples is provided and discussed in detail. It is shown that our results are in agreement with those published in the literature for simpler systems. Further capabilities of the theory are demonstrated on a system containing a buried ferromagnetic layer with periodic magnetic domains.

DOI: 10.1103/PhysRevB.68.144401 PACS number(s): 75.70.Ak, 42.65.Ky

I. INTRODUCTION

Magnetization-induced second-harmonic generation (MSHG) has recently been attracting the attention of many theoretical and experimental studies.[1–11] This is mostly due to the fact that it provides a unique experimental tool for studying the magnetic properties of interfaces in ultrathin magnetic structures.

As follows from various experimental evidence, the *main* contribution to the second-harmonic (SH) field generated in a multilayer system comprised of centrosymmetric materials originates at the layer interfaces, where the local point symmetry of the structure is broken. The model which provides the theoretical background and is widely used for the analysis of the MSHG experiments carried out on such systems was developed by Wierenga *et al.*[1] The model introduces an infinitely thin polarization sheet which acts as a source of the SH field. The sheet is located at an interface of layers comprising the multilayer structure and is considered to be surrounded by infinitely thin vacuum layers. The polarization of the sheet is determined solely by the fundamental electric field at the interface, i.e.,

$$\boldsymbol{P}^{(2\omega)} = \chi \otimes \boldsymbol{E}^{(\omega)} \boldsymbol{E}^{(\omega)}. \tag{1}$$

In this expression, $\boldsymbol{E}^{(\omega)}$ denotes the complex amplitude of the electric field at the fundamental frequency ω at the interface, and χ is the third rank nonlinear susceptibility tensor (the elements of the tensor χ are denoted by χ_{ijk}) which phenomenologically describes the origins of the electromagnetic (EM) field at 2ω.

From the classical EM theory it follows that the introduction of such a polarization sheet implies a discontinuity of the tangential components of the EM field across the interface. Applying this fundamental step along with the matrix formalism relating the EM field across the multilayer system to that outside of the structure, the model developed by Wierenga *et al.*[1] is able to relate the radiated SH field to the intrinsic nonlinear properties of the interface, which are encountered in the values of the susceptibility tensor χ_{ijk}.

The main assumption of the model is that it considers the source of the SH field in the form of an infinitely thin, *coherently* and *homogeneously* polarized sheet. Although this assumption is justifiable in many cases investigated experimentally, it is not sufficiently general. Moreover, it is based on a macroscopic like description of the source of the SH field, which does not provide a direct physical insight into the processes involved in the SHG phenomena.

In our model, we look at the problem of the SHG from a different point of view, which can be better related to the

microscopic description of the origin of the SH field. We consider that the SH field is generated by a *point* electric *dipole* oscillating at an angular frequency 2ω. Although the dipole can be positioned arbitrarily throughout the multilayer structure, we assume that it is placed *at* the layer interface. This is closely related to the symmetry considerations used in the macroscopic models like that discussed above.

The complex amplitude and the orientation of the point dipole are derived from the fundamental EM field at the interface in a similar manner as in Eq. (1), i.e.,

$$\boldsymbol{\mu}^{(2\omega)} = \tilde{\chi} \otimes \boldsymbol{E}^{(\omega)} \boldsymbol{E}^{(\omega)}. \tag{2}$$

This is justified by the fact that our microscopic description, which is based on this equation, should be consistent with the macroscopic description based on Eq. (1).

This approach to the SHG has some advantages. In particular, once the EM field generated by the point dipole (2) is known, it can be used to evaluate the SH field generated from a system with *arbitrarily* spatially distributed dipoles. Furthermore, as it is based on a well understood microscopic quantity (an elementary dipole), it can be more directly related to a quantum-mechanical description of the SHG.

In the models describing the SHG, the symmetry of the interfaces generating the SH field plays a fundamental role. In particular, one can deduce zero and nonzero elements of the nonlinear susceptibility tensor χ_{ijk} from symmetry considerations of the interface microscopic structure. Furthermore, if the local magnetization of the interface is taken into account, the symmetry of the interface is lowered, resulting in an increased number of nonzero elements of χ_{ijk}. The details of this analysis are thoroughly studied in the literature.[12,13] To adopt the symmetry considerations in our description, we assume that the symmetry properties of the tensor $\tilde{\chi}_{ijk}$ in Eq. (2) are identical to those of χ_{ijk} in Eq. (1). In other words, the microscopic point dipole $\boldsymbol{\mu}^{(2\omega)}$, which is the fundamental quantity considered in our analysis, has to fulfill the same symmetry-induced constraints as the macroscopic quantity $\boldsymbol{P}^{(2\omega)}$ used in the previously developed models. Due to this formal equivalence, the tilde in $\tilde{\chi}_{ijk}$ will be omitted throughout this work.

The analysis in this paper proceeds as follows. In Sec. II we present a complete and comprehensive theory of propagation of radiation generated by point electric dipoles embedded within an arbitrary multilayer system. Since the aim of this work is to develop a concise formalism, the derivations start at the very basics of the electromagnetic theory, i.e., the Maxwell equations. Firstly, we introduce the so-called $\boldsymbol{q}$ space in which our problem can be solved in a rather elegant way. We derive a matrix formalism which allows us to obtain analytical expressions for the fundamental field at each interface of the multilayer system. These expressions are then applied in an evaluation of point electric dipoles which generate the second harmonic field. In a subsequent part of the paper, we provide a detailed study of the boundary conditions that the electromagnetic field must fulfill in the vicinity of a point electric dipole. We show how these conditions can be expressed in the above mentioned $\boldsymbol{q}$ space, and how they can be incorporated into the matrix formalism describing the propagation of the second harmonic field across the multilayer structure. The theoretical analysis culminates at the point where the expressions for the angular distribution of the observable SH intensity are derived. A schematic block diagram depicting the flow of the developed formalism is shown in Fig. 1.

In Sec. III we illustrate the theory in a number of numerical examples which are closely related to the magnetic-induced second harmonic generation, which is the main application field of the theory presented in this paper. The final remarks and conclusions are summarized in Sec. IV.

II. THEORY

A. Basic assumptions and conventions

A typical configuration of a SHG experiment carried out on a multilayer system is shown in Fig. 2(a). It employs a fundamental (ω) beam which impinges from the superstrate onto a sample at an incident angle $\theta_0^{(\omega)}$. The reflected and transmitted fundamental light beams are observed in the superstrate and substrate at angles $\theta_0^{(\omega)}$ and $\theta_{M+1}^{(\omega)}$, respectively. The SH (2ω) field generated within the sample is radiated into the superstrate and substrate, where it can be observed at angles $\theta_0^{(2\omega)}$ and $\theta_{M+1}^{(2\omega)}$, respectively. The purpose of the following analysis is to find a relation between the incident fundamental field and the radiated SH field as a function of the incident and observation angles $\theta_0^{(\omega)}$ and $\theta_0^{(2\omega)}$ (or/and $\theta_{M+1}^{(2\omega)}$), respectively.

Throughout the paper, we accommodate the following conventions. Without a loss of generality, we assume a coordinate system in which the incident light beam at the fundamental frequency ω propagates in the y-z plane, as shown in Fig. 2. The x axis is perpendicular to the y and z axes in such a way that they form a right-handed system of coordinates. The unity vectors in the direction of the x, y, and z axes are denoted by $\hat{\boldsymbol{x}}$, $\hat{\boldsymbol{y}}$, and $\hat{\boldsymbol{z}}$, respectively. Furthermore, the time dependence of the field is considered in the form of $\exp[-i\omega_0 t]$, where $\omega_0 = \omega$ and $\omega_0 = 2\omega$ for the fundamental and SH fields, respectively.

The evaluation of the SH field generated within the multilayer system consists of two parts. First, the fundamental field at each interface of the multilayer system is calculated. This field is then used to ''generate'' a point dipole oscillating at a frequency 2ω in a manner described by expression (2). Subsequently, the radiation of such a dipole within the multilayer structure is determined. Finally, the total SH field radiated into the substrate and superstrate is obtained as a sum of the single dipole contributions, which are integrated over the illuminated area and summed over all interfaces.

B. Maxwell equations

In order to find the spatial distribution of the field radiated by a point electric dipole, one needs to solve the Maxwell equations. Considering the above mentioned convention for the time-variations of the electromagnetic field, these equations can be written in the following form:

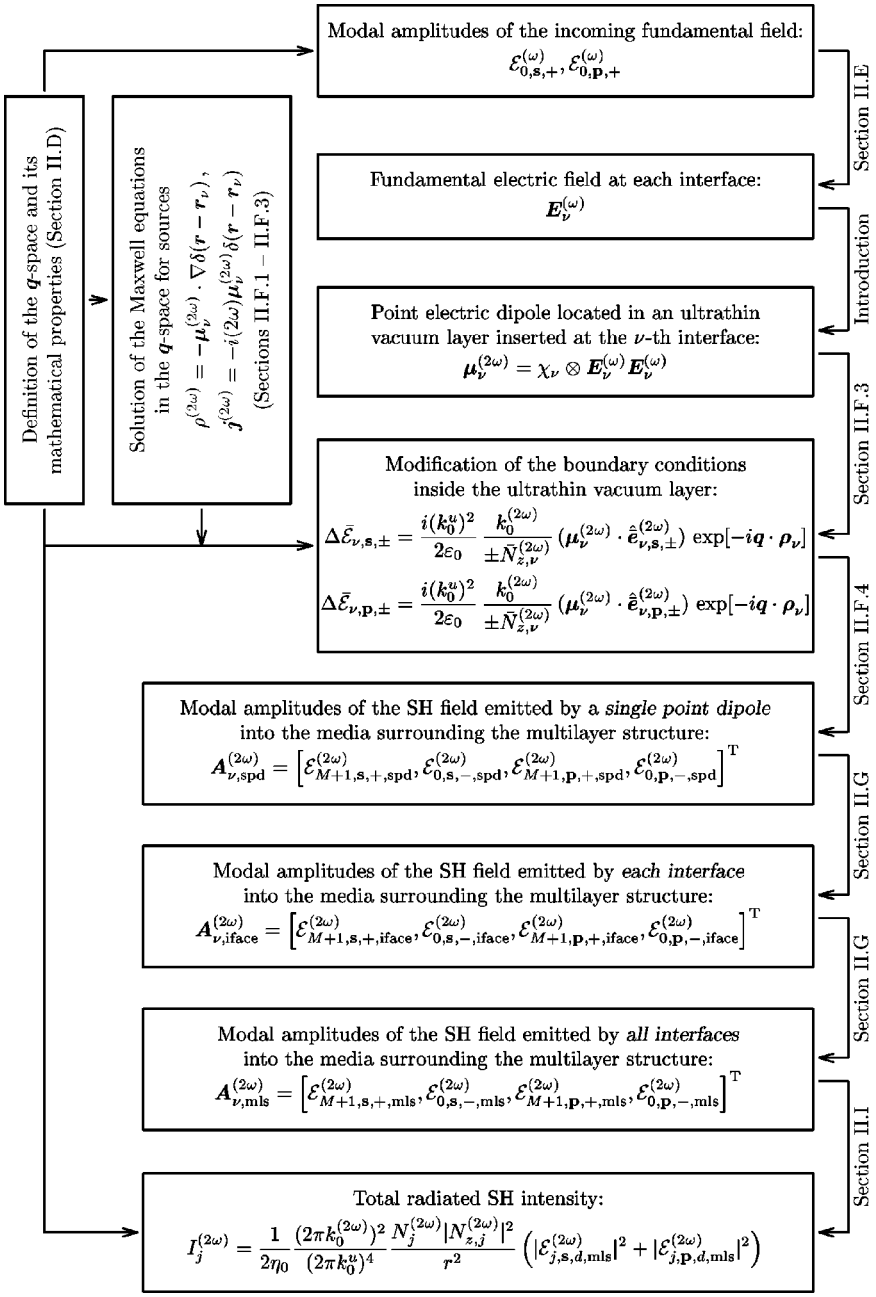

FIG. 1. A schematic diagram of the developed SHG formalism.

$$\nabla\cdot\boldsymbol{D}^{(\omega_0)}=\rho^{(\omega_0)} \quad \text{(a)}, \qquad \nabla\times\boldsymbol{E}^{(\omega_0)}=i\omega_0\boldsymbol{B}^{(\omega_0)} \quad \text{(b)},$$
$$\nabla\cdot\boldsymbol{B}^{(\omega_0)}=0 \quad \text{(c)}, \qquad \nabla\times\boldsymbol{H}^{(\omega_0)}=\boldsymbol{j}^{(\omega_0)}-i\omega_0\boldsymbol{D}^{(\omega_0)} \quad \text{(d)}. \tag{3}$$

In these equations, all the quantities are considered to be functions of the position in the direct space, i.e., $\boldsymbol{E}^{(\omega_0)} \equiv \boldsymbol{E}^{(\omega_0)}(\boldsymbol{r})$, $\boldsymbol{H}^{(\omega_0)} \equiv \boldsymbol{H}^{(\omega_0)}(\boldsymbol{r})$, etc.

The optical properties of the medium can be described by the permittivity, $\boldsymbol{\epsilon}^{(\omega_0)}$, and permeability, $\mu^{(\omega_0)}$, where $\omega_0=\omega$ and $\omega_0=2\omega$ for the fundamental and SH fields, respectively. These quantities relate the field vectors as $\boldsymbol{D}^{(\omega_0)}=\boldsymbol{\epsilon}_0\boldsymbol{\epsilon}^{(\omega_0)}\boldsymbol{E}^{(\omega_0)}$ and $\boldsymbol{B}^{(\omega_0)}=\mu^{(\omega_0)}\boldsymbol{H}^{(\omega_0)}$, where $\boldsymbol{\epsilon}_0$ is the vacuum permittivity and $\boldsymbol{\epsilon}^{(\omega_0)}$ is, in general, a tensor whose elements can be complex numbers (see below for more details). On the other hand, all the media in this article are assumed to be magnetically inactive within the frequency range (optical frequencies) considered in this paper, and therefore the permeability is taken to be equal to the vacuum permeability, i.e., $\mu^{(\omega_0)}\equiv\mu_0$.

The quantities $\rho^{(\omega_0)}$ and $\boldsymbol{j}^{(\omega_0)}$ describe the spatial density of free charges and currents, respectively. For the fundamental frequency, $\omega_0=\omega$, both quantities are considered to be zero everywhere. On the other hand, these quantities are considered to be zero only almost everywhere for $\omega_0=2\omega$, i.e., they act as sources of the SH field.[14] More details on where exactly these quantities are nonzero and how this determines the spatial distribution of the SH electromagnetic field will be provided later on.

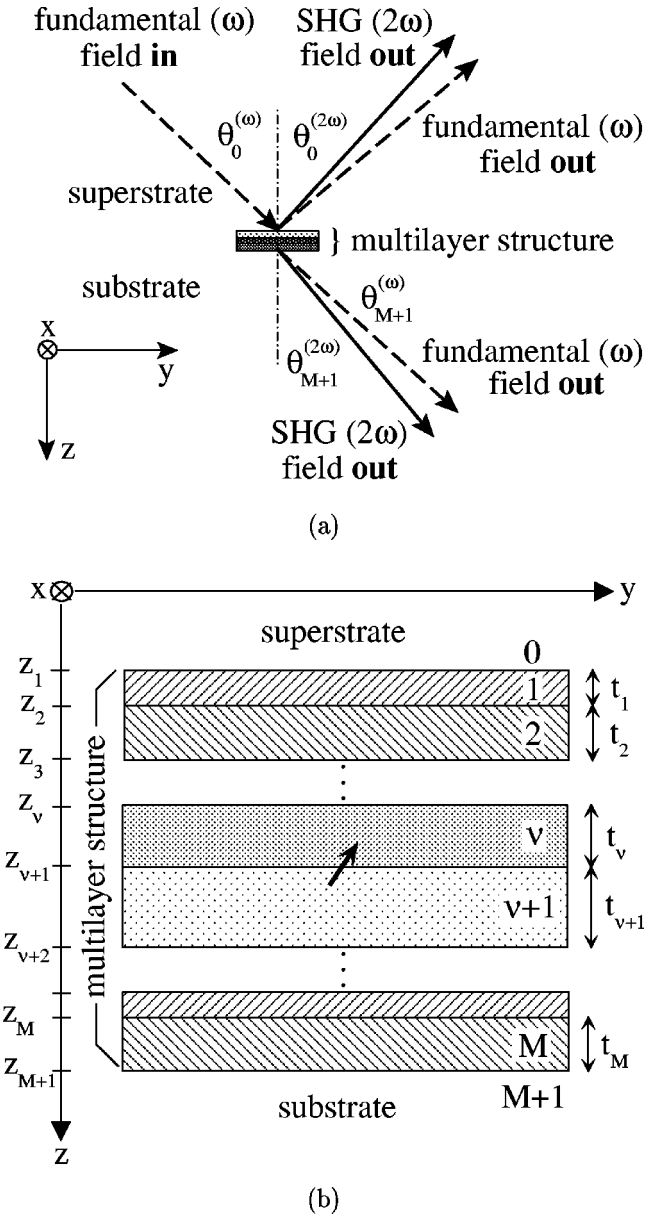

FIG. 2. (a) A diagram of a typical experimental configuration for measuring the second harmonic generation (SHG) from a sample illuminated by a beam at fundamental frequency ω. (b) A schematic diagram of the multilayer structure under consideration, which consists of M homogeneous layers surrounded by a semifinite substrate and superstrate. The positions of the interfaces are characterized by z_ν, $\nu=1,\ldots,M+1$. The thick arrow symbolizes a point dipole located at the $(\nu+1)$th interface and oscillating at an angular frequency 2ω.

C. Multilayer structure

The structure under consideration is a multilayer system consisting of M layers surrounded by a semi-infinite substrate and superstrate, as depicted in Fig. 2(b). Optical properties of the layers are assumed to be uniform in the lateral directions, i.e., described by the permittivity tensors $\epsilon_{ij,\nu}^{(\omega_0)}$, $\nu=0,\ldots,M+1$, which do not vary with the lateral (x and y) coordinates. Throughout the paper, the values of the permittivity tensors are assumed to be normalized to the vacuum permittivity ϵ_0. Since the elements of the permittivity tensors are generally complex, the analysis presented in this work can cover a very broad range of materials, e.g., isotropic or anisotropic dielectrics, absorbing media, metals, and magneto-optical materials.

The interfaces between the layers are assumed to be planar and parallel to the x-y plane. They are located at positions $z_1, z_2, \ldots, z_{M+1}$, which can be calculated from the thicknesses of the layers as $z_\nu = z_1 + t_1 + \cdots + t_{\nu-1}$, $\nu = 1,\ldots,M+1$, as shown in Fig. 2(b).

It is important to note that the *macroscopic* optical response of the layers comprising the multilayer system is considered to be *linear* at both the fundamental and SH frequencies. That is to say that the fundamental and SH vector fields present in the multilayer structure propagate according to the laws dictated by the spatial distribution of the permittivity tensors $\boldsymbol{\epsilon}^{(\omega_0)}$ (Ref. 15) *and* the linear relation between the vectors $\boldsymbol{D}^{(\omega_0)}$ and $\boldsymbol{E}^{(\omega_0)}$, i.e., $\boldsymbol{D}^{(\omega_0)} = \epsilon_0 \boldsymbol{\epsilon}^{(\omega_0)} \boldsymbol{E}^{(\omega_0)}$, for both the fundamental ($\omega_0 = \omega$) and second harmonic ($\omega_0 = 2\omega$) fields. The existence of the SH field in such media is solely a consequence of the *microscopic* properties of the layer *interfaces*, which exhibit nonlinearity as described in Sec. I. This nonlinearity is, however, described separately, i.e., as a property inherent to the interfaces rather than to the media comprising the multilayer systems. In particular, the nonlinear properties of each interface are characterized by the nonlinear susceptibility tensor $\chi_{ijk,\nu}$, where the subscript ν refers to the interface located at z_ν [see Fig. 2(b)].

Each nonlinearity tensor can be decomposed into parts $\chi_{ijk,\nu}^{(o)}$ and $\chi_{ijk,\nu}^{(e)}$, which are odd and even in magnetization, respectively. The exact form of the tensors, namely, which elements are zero or nonzero, can be derived when both the structural microscopic symmetry and the local magnetization at each interface are considered. This analysis was thoroughly studied and reported in the literature for various microscopic structures,[12,13] and the results will be used later on in a section providing numerical examples.

In summary of this section, in this work we consider multilayer structures comprised of parallel layers whose optical properties (i.e., permittivity tensors) are laterally homogeneous but whose interfaces are characterized by possibly laterally inhomogeneous nonlinearity tensors $\chi_{ijk,\nu} \equiv \chi_{ijk,\nu}(x,y)$. Such situations can be encountered in multilayer structures with magnetic domains, spin waves, etc. Other interesting situations include, for example, laterally designed arrays of magnetic nanostructures for which the above mentioned assumptions (the lateral homogeneity of the optical properties) are fulfilled, such as arrays of dots designed e.g. by (i) uniform He ion irradiation through a mask, which maintains the planarity far below one nanometer,[16] (ii) focused Ga ion beam irradiation, where dots are separated by paramagnetic irradiated sharp and quasiunetched lines,[17,18] or (iii) magnetic film deposition on a weakly patterned substrate.[19]

D. Decomposition of the fundamental field in a homogeneous unbound medium

The principle aim of the analysis of the field distribution across a multilayer structure is to find functions $\boldsymbol{E}^{(\omega_0)}(\boldsymbol{r})$ and

$\boldsymbol{H}^{(\omega_0)}(\boldsymbol{r})$ describing the fundamental ($\omega_0=\omega$) and SH ($\omega_0=2\omega$) electric and magnetic fields in the direct ($\boldsymbol{r}$) space, respectively. However, due to the properties of the Fourier transform, a satisfactory description, which is in fact more advantageous for the description of the SHG experiments described above, is achieved by finding the functions $\boldsymbol{\mathcal{E}}^{(\omega_0)}(\boldsymbol{k}^{(\omega_0)})$ and $\boldsymbol{\mathcal{H}}^{(\omega_0)}(\boldsymbol{k}^{(\omega_0)})$ describing the electric and magnetic fields in the Fourier ($\boldsymbol{k}$) space, respectively. For the purpose of clarity, the superscript ω_0 will be omitted in the following derivations, unless absolutely necessary. The field descriptions in the direct and Fourier spaces, which in the following analysis are called the $\boldsymbol{r}$ space and the $\boldsymbol{k}$ space, respectively, are related by the inverse Fourier transform, i.e.,

$$\boldsymbol{E}(\boldsymbol{r})=\frac{1}{(2\pi)^3}\frac{1}{(k_0^u)^3}\int\int\int \mathrm{d}^3\boldsymbol{k}\boldsymbol{\mathcal{E}}(\boldsymbol{k})\exp[i\boldsymbol{k}\cdot\boldsymbol{r}], \qquad (4)$$

and similarly for $\boldsymbol{H}(\boldsymbol{r})$.[20] In this equation, the factor $(1/k_0^u)^3$ has been formally inserted in order to equalize the units of the fields in the $\boldsymbol{r}$ and $\boldsymbol{k}$ spaces. It can be, in principle, any constant with units m^3, but in this work $(1/k_0^u)^3=(c_0/\omega)^3$, where c_0 is the speed of light in vacuum, is opted for. The integrand in Eq. (4) represents a plane wave propagating in the direction of the wave vector $\boldsymbol{k}$. Because we will treat the electromagnetic field in materials characterized in general by anisotropic and complex permitivity tensors, all the components of the $\boldsymbol{k}$ vector are also considered to be generally complex. As follows from the properties of the generalized Fourier transform, Eq. (4) describes *any* distribution of electric field $\boldsymbol{E}(\boldsymbol{r})$ in an unbound medium, e.g., constant field, field oscillating at different frequencies, and propagating in different directions, or even fields containing discontinuities or sungularities of the type of the Dirac δ function or their derivatives. Consequently, both near and far fields, and even the field at the position of the radiating dipole, are included in the analysis.

Since the plane waves are eigensolutions of the wave equations which can be derived from the Maxwell equations (3), we will also refer to them as the eigenmodes, or just modes. In this context, $\boldsymbol{\mathcal{E}}(\boldsymbol{k})$ represents the vector amplitude of the mode characterized by the direction of propagation equal to $\boldsymbol{k}$ and will therefore be called the *vector modal amplitude*. It should be noted that both $\boldsymbol{E}(\boldsymbol{r})$ and $\boldsymbol{\mathcal{E}}(\boldsymbol{k})$ are assumed to be generally complex three-dimensional (3D) vectors, as a consequence of both a complex representation of the time dependance[21,22] and a generally complex form of the permittivity tensors describing the optical properties of the involved media.

The general equation (4) can be simplified if the field is assumed to be monochromatic, i.e., oscillating at a single frequency ω_0. In this case, the integration over the entire three-dimensional complex $\boldsymbol{k}$ space is reduced to the integration over a two-dimensional complex area $\boldsymbol{k}(\omega_0)$, where ω_0 is a constant. This area is determined by the optical properties of the material in which the field propagates and can be found by solving the Maxwell equations. For example, in an isotropic medium characterized by a scalar dielectric permittivity ϵ, the integration is performed over a complex sphere of a complex radius $k^{(\omega_0)}=\sqrt{\boldsymbol{k}^{(\omega_0)}\cdot\boldsymbol{k}^{(\omega_0)}}=\sqrt{\epsilon}(\omega_0/c_0)$, where $\mathrm{Re}(k^{(\omega_0)})>0$ is assumed. In a more general case, i.e., for an anisotropic medium characterized by the permittivity tensor ϵ_{ij}, the situation is more complicated because the length of the vector $\boldsymbol{k}$ also depends on the direction of the $\boldsymbol{k}$ vector and the polarization of the propagating light. In any case, it can be said that due to monochromaticity of the field, the k_x, k_y, and k_z components of the $\boldsymbol{k}$ vector are related to each other. Consequently, the k_z-component can be expressed as a function of the remaining k_x and k_y components, angular frequency, and material parameters, i.e.,

$$k_{z,p,d}\equiv k_{z,p,d}(k_x,k_y,\omega_0,\epsilon_{ij}), \qquad (5)$$

where k_x and k_y are generally complex. The index p, which takes the values 1 or 2, represents the fact that there exist two orthogonally polarized modes whose k_z can be, in general, different. Furthermore, the index d represents the z direction of the $\boldsymbol{k}$ vector. In this work, we use $d=+$ and $d=-$ to denote modes propagating in the positive $[\mathrm{Re}(k_z)>0]$ and negative $[\mathrm{Re}(k_z)<0]$ z directions, respectively. In summary, for given values of k_x, k_y, and ω_0, there exist four modes of the electromagnetic field propagating in the medium characterized by the permittivity tensor ϵ_{ij}. The corresponding vector modal amplitudes will be denoted as $\boldsymbol{\mathcal{E}}_{\boldsymbol{k},p,d}(\boldsymbol{k})$, where the subscript $\boldsymbol{k}$ indicates that the amplitudes are expressed in the $\boldsymbol{k}$ space.

1. Definition of the q space

As discussed above, the consequence of the monochromaticity is that k_z is not a free parameter. Thus a particular *light mode* (propagating in a given material and oscillating at a given frequency) is fully described by a two-dimensional, generally complex vector $\boldsymbol{q}=[k_x,k_y]$. Such a light mode consists of four plane waves, each propagating in a direction given by $\boldsymbol{k}_{p,d}=[\boldsymbol{q},k_{z,p,d}]$. Thus, an arbitrary spatial distribution of the monochromatic electric field $\boldsymbol{E}(\boldsymbol{r})$ can be expressed as an integral over all light modes, each parametrized by a single vector $\boldsymbol{q}\equiv[k_x,k_y]$, i.e.,

$$\boldsymbol{E}(\boldsymbol{r})=\frac{1}{(2\pi)^2}\frac{1}{(k_0^u)^2}\int\int \mathrm{d}^2\boldsymbol{q}\sum_{p=1,2}\sum_{d=\pm}\boldsymbol{\mathcal{E}}_{\boldsymbol{q},\nu,p,d}\exp[i\boldsymbol{q}\cdot\boldsymbol{\rho}], \qquad (6)$$

where $\boldsymbol{\rho}\equiv[x,y]$. This equation provides the description of the field in the newly defined $\boldsymbol{q}$ space. The subscript $\boldsymbol{q}$ in the vector modal amplitudes $\boldsymbol{\mathcal{E}}_{\boldsymbol{q},\nu,p,d}$ indicates that these quantities are expressed in this $\boldsymbol{q}$ space.

It is important to realize that these vector amplitudes depend explicitly on the z coordinate, which is clear from a direct comparison of Eqs. (4) and (6). In this paper we deal with a multilayer system with interfaces located at positions z_ν. Consequently, we have chosen to use the subscript ν in $\boldsymbol{\mathcal{E}}_{\boldsymbol{q},\nu,p,d}$ to denote the vector modal amplitude of the field inside the νth layer at the location infinitesimally close to the νth interface, i.e., at the location $z=z_\nu+\epsilon$ where $\epsilon\to 0$, as depicted in Fig. 3. The only exception is the vector modal amplitude $\boldsymbol{\mathcal{E}}_{\boldsymbol{q},0,p,d}$ in the superstrate ($\nu=0$), which corre-

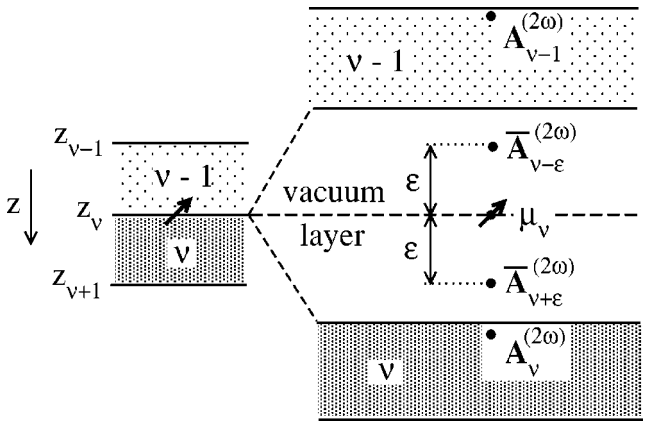

FIG. 3. A schematic diagram depicting an oscillating point dipole located inside an infinitesimally thin vacuum layer inserted at the position of the νth interface. Note the position (dark point) of the vector $\boldsymbol{A}^{(2\omega)}_{\nu}=[\mathcal{E}^{(2\omega)}_{\nu,1,+},\mathcal{E}^{(2\omega)}_{\nu,1,-},\mathcal{E}^{(2\omega)}_{\nu,2,+},\mathcal{E}^{(2\omega)}_{\nu,2,-},]^T$ which is defined to be located inside the νth layer in the vicinity of the νth interface.

sponds to the field in the superstrate in the vicinity of the first interface, as there is no zeroth interface. In the following analysis, the Maxwell equations together with the boundary conditions will be treated in the $\boldsymbol{q}$ space, as it matches exactly the characteristics of a space in which the field propagating across a multilayer system should be considered.

(i) The $\boldsymbol{q}$ space is monochromatic, meaning that it provides a framework for the description of the field oscillating at one single frequency ω.

(ii) The $\boldsymbol{q}$ space comprises a 2D Fourier space, obtained as a Fourier image of the x-y plane, and a 1D direct space in the z direction. Hence the $\boldsymbol{q}$ space reflects the fact that the optical properties of the multilayer system vary only in the z direction.

(iii) As follows from the properties of the Fourier transform, the $\boldsymbol{q}$ space allows the description of *any* spatial distribution of complex $\boldsymbol{E}(\boldsymbol{r})$ in a multilayer structure (for monochoromatic field). For example, a field corresponding to plane waves or a field with discontinuities and singularities can be described. Thus, similarly to the $\boldsymbol{k}$ space, the $\boldsymbol{q}$ space provides a framework for the description of the field radiated by an electric point dipole in both near and far fields.

(iv) The propagation of a particular light mode is fully characterized by a single, generally complex vector $\boldsymbol{q}=[k_x,k_y]$. To each vector $\boldsymbol{q}$ corresponds a set of four plane waves, each characterized by a different value of k_z given by Eq. (5). Amplitudes of these waves are described by four, generally complex, vector modal amplitudes $\boldsymbol{\mathcal{E}}_{\boldsymbol{q},\nu,p,d}$. For example, as will be shown later (Sec. II D 3 a), if only one light mode is present in the multilayer structure (such as in a case of a light wave entering the multilayer structure at a single angle of incidence), these four amplitudes are proportional to Dirac δ functions, each of them located in the same point of the $\boldsymbol{q}$ space. On the other hand, if the light is propagating through the multilayer system in many directions (such as in a case of the radiation of an electric point dipole, as discussed in Sec. II F), the vector modal amplitudes are described by smooth functions in the k_x and k_y coordinates.

(v) It will be shown later that the radiation originating from an electric point dipole can be in the $\boldsymbol{q}$ space described by a smooth function [see Eq. (67)], in contrast to the $\boldsymbol{k}$ space, where the radiated field is described by a diverging function.[23,24]

Since all the quantities will be considered in the $\boldsymbol{q}$ space, the subscript $\boldsymbol{q}$ will be often omitted. In the subsequent derivations, the vector modal amplitudes $\boldsymbol{\mathcal{E}}_{\nu,p,d}$ will be considered in one of the following forms:

$$\boldsymbol{\mathcal{E}}_{\nu,p,d}\equiv\begin{bmatrix}\mathcal{E}_{x,\nu,p,d}\\ \mathcal{E}_{y,\nu,p,d}\\ \mathcal{E}_{z,\nu,p,d}\end{bmatrix}\equiv\mathcal{E}_{\nu,p,d}\hat{\boldsymbol{e}}_{\nu,p,d}. \tag{7}$$

The quantities $\mathcal{E}_{\nu,p,d}$ and $\hat{\boldsymbol{e}}_{\nu,p,d}$, where $|\hat{\boldsymbol{e}}_{\nu,p,d}|=1$, will be referred to as the *modal magnitude* and the *modal polarization*, respectively. In this context it is important to distinguish between the subscript z, which denotes the z component of the vector modal amplitude, and ν, which corresponds to the location of the $\boldsymbol{q}$ space at $z=z_\nu+\epsilon$, $\epsilon\rightarrow 0$.

The vector modal amplitudes $\boldsymbol{\mathcal{E}}_{\nu,p,d}$ will often appear as a sum over either the polarization index p or the direction index d, or both. Therefore, it will become useful to introduce the "summing index" Σ as follows:

$$\begin{aligned}\boldsymbol{\mathcal{E}}_{\nu,p,\Sigma}&=\sum_{d=\pm}\boldsymbol{\mathcal{E}}_{\nu,p,d},\\ \boldsymbol{\mathcal{E}}_{\nu,\Sigma,d}&=\sum_{p=1,2}\boldsymbol{\mathcal{E}}_{\nu,p,d},\\ \boldsymbol{\mathcal{E}}_{\nu,\Sigma,\Sigma}&=\sum_{d=\pm}\sum_{p=1,2}\boldsymbol{\mathcal{E}}_{\nu,p,d}.\end{aligned} \tag{8}$$

For example, $\boldsymbol{\mathcal{E}}_{\nu,\Sigma,\Sigma}$, being the sum of all vector modal amplitudes, represents the electrical field at position z_ν expressed in the $\boldsymbol{q}$ space, as follows from Eq. (6). Applying the properties of the Fourier transform and definition (6), $\boldsymbol{\mathcal{E}}_{\nu,\Sigma,\Sigma}$ can be calculated from the field distribution in the direct space using the equation

$$\boldsymbol{\mathcal{E}}_{\nu,\Sigma,\Sigma}(\boldsymbol{q},z_\nu)=(k_0^u)^2\int\int \mathrm{d}^2\boldsymbol{\rho}\,\boldsymbol{E}(\boldsymbol{\rho},z_\nu)\exp[-i\boldsymbol{\rho}\cdot\boldsymbol{q}]. \tag{9}$$

2. Relation between the q and k spaces in an isotropic medium

As follows from the comparison of Eqs. (4) and (6), the relation between the $\boldsymbol{k}$ and $\boldsymbol{q}$ spaces is obtained by the integration over k_z. For a mode in the $\boldsymbol{q}$ space one can write

$$\boldsymbol{\mathcal{E}}_{\nu,\Sigma,\Sigma}=\frac{1}{2\pi}\frac{1}{k_0^u}\int \mathrm{d}k_z\boldsymbol{\mathcal{E}}_{\boldsymbol{k}}(\boldsymbol{k})\exp[ik_z z_\nu]. \tag{10}$$

As mentioned earlier, the EM field is assumed to be monochromatic, i.e., oscillating at a frequency ω_0. In the context of Eq. (10) this means that the function $\boldsymbol{\mathcal{E}}_{\boldsymbol{k}}(\boldsymbol{k})$ in the $\boldsymbol{k}$ space can be written as

$$\boldsymbol{\mathcal{E}}_{\boldsymbol{k}}(\boldsymbol{k})=\sum_{p=1,2}\boldsymbol{\mathcal{E}}_{\boldsymbol{k},p}(\boldsymbol{k})\,\delta(\tilde{\omega}-\omega_0)\,\omega_0. \tag{11}$$

In other words, the vector modal amplitude of the plane waves is nonzero only for such angular frequencies $\tilde{\omega}$ ($\tilde{\omega}$ denotes *all* possible frequencies) for which the equation $\tilde{\omega} = \omega_0$ is valid. The factor ω_0 in Eq. (11) was inserted in order to make the units of the vector amplitudes at the left-hand and right-hand sides equal.

A more suitable form of the relation between the vector modal amplitudes expressed in the $\boldsymbol{k}$ space and the $\boldsymbol{q}$ space is obtained when the integration over k_z is carried out. We recall that during this integration the following relations should be carefully considered.

(a) In the $\boldsymbol{k}$ space, the condition $\tilde{\omega} = \omega_0$ is fulfilled for four values of k_z, namely those expressed by Eq. (5). In the case of an isotropic medium characterized by a scalar permittivity ϵ_ν, these four values are reduced to two. In particular, the values of $k_{z,\nu,p,d}$ are equal for both polarization states $p = 1,2$, and have opposite signs for the direction indices $d = +$ and $d = -$, i.e.,

$$k_{z,\nu,p,\pm} = \pm k_{z,\nu}, \tag{12}$$

where

$$k_{z,\nu} = \sqrt{k_\nu^2 - k_x^2 - k_y^2}, \quad k_\nu = \sqrt{\epsilon_\nu} k_0^{(\omega_0)} = \sqrt{\epsilon_\nu}(\omega_0/c_0). \tag{13}$$

In the general case of an anisotropic medium, the situation is more complicated, but since we are interested in the relation between the $\boldsymbol{k}$ and $\boldsymbol{q}$ spaces only in an isotropic medium, this issue will not be dealt with in detail here.

(b) The term $\tilde{\omega} - \omega_0$ in the argument of the δ function can be formally rearranged as[25]

$$\tilde{\omega} - \omega_0 = \frac{\tilde{\omega}^2 - \omega_0^2}{\tilde{\omega} + \omega_0} = \frac{c_0}{\sqrt{\epsilon_\nu}} \frac{k^2 - k_\nu^2}{k + k_\nu} = \frac{c_0}{\sqrt{\epsilon_\nu}} \frac{k_z^2 - k_{z,\nu,p,d}^2}{k + k_\nu}. \tag{14}$$

In this equation, k and k_z represent *all* possible values of the magnitude and z component of the $\boldsymbol{k}$ vector, respectively, and are related to $\tilde{\omega}$ through expressions $\tilde{\omega}/c_0 = k/\sqrt{\epsilon_\nu}$ and $k_z^2 = k^2 - k_x^2 - k_y^2$. The last step in Eq. (14) is of particular importance as it provides a relation between k_z and $\tilde{\omega}$ which appear in Eqs. (10) and (11), respectively.

Considering relations (11) and (14), integration (10) can be performed and the relation between the vector modal amplitudes in the $\boldsymbol{q}$ and $\boldsymbol{k}$ spaces can be written as

$$\boldsymbol{\mathcal{E}}_{\nu,p,\pm} \equiv \boldsymbol{\mathcal{E}}_{\boldsymbol{q},\nu,p,\pm} = \frac{1}{2\pi} \sqrt{\epsilon_\nu} \frac{k_0^{(\omega_0)}}{k_0^u} \frac{k_\nu}{k_{z,\nu,p,\pm}} \boldsymbol{\mathcal{E}}_{\boldsymbol{k},p}(\boldsymbol{k}_{\nu,p,\pm}) \exp[\pm i k_{z,\nu} z_\nu], \tag{15}$$

where the vector $\boldsymbol{k}_{\nu,p,\pm}$ is defined as

$$\boldsymbol{k}_{\nu,p,\pm} = [k_x, k_y, k_{z,\nu,p,\pm}], \tag{16}$$

and its z component $k_{z,\nu,p,\pm}$ is given by Eq. (12). Applying the same steps as above, similar relations can be found for all other field quantities, i.e., for $\boldsymbol{D}$, $\boldsymbol{H}$ and $\boldsymbol{B}$, whose equivalents in the $\boldsymbol{q}$ space are denoted as $\boldsymbol{\mathcal{D}}$, $\boldsymbol{\mathcal{H}}$, and $\boldsymbol{\mathcal{B}}$, respectively.

3. Some useful properties of the q space

In the following sections, we will find a solution to the Maxwell equations (3) which corresponds to a source taking the form of an electric point dipole oscillating at an angular frequency $\omega_0 = 2\omega$. Since the point dipole will be described by means of the Dirac δ function, it is necessary to study the properties of the $\boldsymbol{q}$ space in the broader sense, i.e., in the sense of distributions (generalized functions).

From the fundamental properties of the Fourier transform it follows that an *arbitrary* two-dimensional distribution of the field across the x-y plane located at $z = z_\nu$, i.e., the function $\boldsymbol{E}(x,y,z_\nu)$, can be described in the $\boldsymbol{q}$ space by the corresponding function $\boldsymbol{\mathcal{E}}_{\nu,p,d}(\boldsymbol{q})$. The word "arbitrary" refers to the fact that even if the field in the direct 2D space contains discontinuities or even singularities of the type of the Dirac δ functions or its derivatives, its description in the $\boldsymbol{q}$ space can always be found. Below, we demonstrate a few examples which will be relevant in the analysis presented in the following sections.

(a) *Monochromatic plane wave.* A monochromatic plane wave propagating in the direction of the wave-vector $\boldsymbol{k}_0 = [k_{x0}, k_{y0}, k_{z0}]$ is described in the direct space as $\boldsymbol{E}(\boldsymbol{r}) = \boldsymbol{E}_0 \exp[ik_{x0}x + ik_{y0}y + ik_{z0}z]$. Inserting this expression into Eq. (6), one can find the following: (i) If $k_{z0} > 0$, i.e., $k_{z,\nu,p,+} \equiv k_{z0}$, then the vector modal amplitudes in the $\boldsymbol{q}$ space are equal to $\boldsymbol{\mathcal{E}}_{\nu,\Sigma,+} = \boldsymbol{E}_0 \delta(\boldsymbol{q} - \boldsymbol{q}_0)(2\pi k_0^u)^2 \exp[ik_{z0}z_\nu]$ and $\boldsymbol{\mathcal{E}}_{\nu,\Sigma,-} = 0$. (ii) If $k_{z0} < 0$, i.e., $k_{z,\nu,p,-} \equiv k_{z0}$, then the vector modal amplitudes are equal to $\boldsymbol{\mathcal{E}}_{\nu,\Sigma,-} = \boldsymbol{E}_0 \delta(\boldsymbol{q} - \boldsymbol{q}_0)(2\pi k_0^u)^2 \exp[ik_{z0}z_\nu]$ and $\boldsymbol{\mathcal{E}}_{\nu,\Sigma,+} = 0$. In both of these expressions, $\boldsymbol{q}_0 = [k_{x0}, k_{y0}]$ was taken.

(b) *Field with discontinuities/singularities in the x dimension.* A field distribution which contains a discontinuity and singularities of the type of the Dirac δ-function and its derivatives in the x dimension can be written as

$$\boldsymbol{E}(x,y,z_\nu) = \Delta\boldsymbol{E}\,\vartheta(x - x_0) + \boldsymbol{E}_\delta \frac{1}{k_0^u} \delta(x - x_0) + \boldsymbol{E}_{\partial\delta} \frac{1}{(k_0^u)^2} \frac{\partial}{\partial x} \delta(x - x_0) + \cdots, \tag{17}$$

where $\vartheta(x - x_0)$ is the Heaviside step function with a step located at $x = x_0$. Consequently, the vector modal amplitudes in the $\boldsymbol{q}$ space can be written as

$$\boldsymbol{\mathcal{E}}_{\nu,\Sigma,\Sigma} = 2\pi \frac{(k_0^u)^2}{ik_x} \delta(k_y) \exp[-ik_x x_0] \times \left(\Delta\boldsymbol{E} + \boldsymbol{E}_\delta \frac{ik_x}{k_0^u} + \boldsymbol{E}_{\partial\delta} \left(\frac{ik_x}{k_0^u} \right)^2 + \cdots \right), \tag{18}$$

as follows from Eq. (6) and the properties of the Fourier transform. This case could straightforwardly be generalized to a case where the discontinuities and singularities are present at more than one point as well as in both the x and y dimensions.

In Eq. (18), the dependence of the vector modal amplitude $\boldsymbol{\mathcal{E}}_{\nu,\Sigma,\Sigma}$ on z is given by the dependence of the quantities $\Delta\boldsymbol{E}$,

$\boldsymbol{E}_{\delta}$, $\boldsymbol{E}_{\partial\delta}$, etc., on z. For every value of z, the field distributions which contain discontinuities or singularities in the x dimension, such as that given by Eq. (17), are expressed by a *continuous* function in the corresponding k_x space. Similar conclusion can be drawn for the field distributions containing discontinuities or singularities in the y dimension. Since the integration over the z dimension is not performed in Eq. (6), the discontinuities/singularities in the z dimension are *conserved* during the transformation between the $\boldsymbol{r}$ space and the $\boldsymbol{q}$ space, and thus need to be treated separately, as shown below.

(c) *Field with a discontinuity/singularity in the z dimension.* A field distribution containing a discontinuity and a δ-type singularity located at the position of the νth interface, i.e., at $z=z_{\nu}$, can be written as

$$\boldsymbol{E}(\boldsymbol{\rho},z)=\{\boldsymbol{E}(\boldsymbol{\rho},z)\}+\Delta\boldsymbol{E}\,\vartheta(z-z_{\nu})+\boldsymbol{E}_{\delta}\frac{1}{k_0^u}\,\delta(z-z_{\nu}), \tag{19}$$

where $\{\boldsymbol{E}(\boldsymbol{\rho},z)\}$ denotes the smooth part of the function and $\boldsymbol{\rho}\equiv[x,y]$. The quantities $\Delta\boldsymbol{E}$ and $\boldsymbol{E}_{\delta}$ represent the magnitudes of the discontinuity and singularity, respectively.

If the discontinuity and singularity are constant with respect to the x and y coordinates, Eq. (19) can be transformed into the $\boldsymbol{q}$ space as

$$\boldsymbol{\mathcal{E}}_{\nu,\Sigma,\Sigma}=\{\boldsymbol{\mathcal{E}}_{\nu,\Sigma,\Sigma}\}+\Delta\boldsymbol{E}(2\pi k_0^u)^2\,\vartheta(z-z_{\nu})\,\delta(\boldsymbol{q})+\boldsymbol{E}_{\delta}(2\pi)^2 k_0^u\,\delta(z-z_{\nu})\,\delta(\boldsymbol{q}). \tag{20}$$

If the discontinuity/singularity is not constant with respect to x and y, the result is formally the same as in Eq. (20) but the term $\delta(\boldsymbol{q})$ is changed accordingly to the variation of the discontinuity/singularity in the x and y directions.

Comparing Eqs. (19) and (20), one can find that the discontinuity of the field around the plane $z=z_{\nu}$, i.e.,

$$\boldsymbol{E}(\boldsymbol{\rho},z_{\nu}+\epsilon)-\boldsymbol{E}(\boldsymbol{\rho},z_{\nu}-\epsilon)=\Delta\boldsymbol{E}, \tag{21}$$

where $\epsilon\rightarrow 0$, is transformed into the $\boldsymbol{q}$ space as

$$\boldsymbol{\mathcal{E}}_{\nu+\epsilon,\Sigma,\Sigma}-\boldsymbol{\mathcal{E}}_{\nu-\epsilon,\Sigma,\Sigma}=(2\pi k_0^u)^2\Delta\boldsymbol{E}\,\delta(\boldsymbol{q}), \tag{22}$$

where $\boldsymbol{\mathcal{E}}_{\nu\pm\epsilon,\Sigma,\Sigma}$ denotes the vector modal amplitude expressed in the $\boldsymbol{q}$ space located at $z=z_{\nu}\pm\epsilon$. This equation implies that the discontinuity of the field distribution across $z=z_{\nu}$ is maintained also in the $\boldsymbol{q}$ space and such a discontinuity is *not* affected by the presence of a singularity in the z dimension located at $z=z_{\nu}$ in the direct space.

In conclusion, we derived two important properties of the $\boldsymbol{q}$ space in this section. We showed that discontinuities/singularities of the field distribution in the x and y dimensions of the $\boldsymbol{r}$ space do not affect the boundary conditions expressed in the $\boldsymbol{q}$ space, and that the boundary conditions in the $\boldsymbol{q}$ space are not affected by the presence of a singularity of the type of Dirac δ function or its derivatives in the z dimension but only by the presence of a field discontinuity in the z direction of the direct space. These properties will be useful in Sec. II F 2 where the boundary conditions in the presence of a radiating point dipole are derived.

E. Distribution of the fundamental field across the multilayer system

Before the SH field generated within the multilayer structure can be found, the fundamental field across the entire multilayer structure has to be evaluated. We assume that the fundamental field is produced by an outside source in a form of a plane electromagnetic wave impinging on the multilayer system in the y-z plane at an angle $\theta_0^{(\omega)}$, as shown in Fig. 2(a). To find the distribution of the field across the multilayer system resulting from such an input condition, the Maxwell equations (3) need to be solved. To do this, we adopt a well-known 4×4 matrix formalism which has been reported in the literature.[26–28]

Since the fundamental field is assumed to originate from an outside source, the charge and current densities at the fundamental frequency are considered to be identically zero everywhere in the multilayer structure, i.e., $\rho^{(\omega)}\equiv 0$ and $\boldsymbol{j}^{(\omega)}\equiv\boldsymbol{0}$ in Eqs. (3a) and (3d). Since each layer comprising the multilayer system is assumed to be homogeneous, the decomposition given by Eq. (4) can be carried out separately for each layer. Furthermore, due to the monochromaticity of the light, the decomposition given by Eq. (6), where the vector modal amplitudes in the $\boldsymbol{k}$ and $\boldsymbol{q}$ spaces are related by Eq. (15), can also be performed separately for each layer.

In the following derivations, normalized wave vectors defined as $\boldsymbol{N}^{(\omega)}\equiv\boldsymbol{k}^{(\omega)}/k_0^{(\omega)}$, where $k_0^{(\omega)}=\omega/c_0$, will be used, as it is more convenient from the point of view of the formalism employed. The normalized wave vector in the νth layer will be denoted by $\boldsymbol{N}_{\nu}^{(\omega)}\equiv\boldsymbol{k}_{\nu}^{(\omega)}/k_0^{(\omega)}$. Due to the coordinate system used, only the y and z components of the normalized wave vector of the fundamental field are nonzero, and will be denoted by $N_{y,\nu}^{(\omega)}$ and $N_{z,\nu}^{(\omega)}$, respectively.

1. Wave equation

When the field vectors in the form of Eq. (6) are substituted into the Maxwell equations (3), the well-known wave equation can be derived. In the νth layer characterized by the permittivity tensor $\epsilon_{ij,\nu}^{(\omega)}$, the wave equation for the electric field takes the form[27]

$$[N_{i,\nu}^{(\omega)}N_{j,\nu}^{(\omega)}+\epsilon_{ij,\nu}^{(\omega)}]\boldsymbol{\mathcal{E}}_{\boldsymbol{q}}^{(\omega)}=(N_{\nu}^{(\omega)})^2\boldsymbol{\mathcal{E}}_{\boldsymbol{q}}^{(\omega)}. \tag{23}$$

An equivalent equation can be derived for all other field vectors. In this equation, $N_{i,\nu}^{(\omega)}$ denotes the ith component of the normalized wave vector $\boldsymbol{N}_{\nu}^{(\omega)}$. The norm of this vector, which is denoted by $N_{\nu}^{(\omega)}$, can be calculated from $(N_{\nu}^{(\omega)})^2=(N_{y,\nu}^{(\omega)})^2+(N_{z,\nu}^{(\omega)})^2$. It is important to notice that the unknowns in the wave equation (23) are the vector modal amplitudes expressed in the $\boldsymbol{q}$ space, which is indicated explicitly by the subscript $\boldsymbol{q}$. This subscript will be, however, omitted in the following derivations. The superscript (ω) indicates that Eq. (23) is the wave equation for the fundamental field.

It should be noted that the form of the wave equation (23) for the vector modal amplitude $\boldsymbol{\mathcal{E}}_{\boldsymbol{q}}$ expressed in the $\boldsymbol{q}$ space is the same as the well-known wave equation for the vector modal amplitude $\boldsymbol{\mathcal{E}}_{\boldsymbol{k}}$ expressed in the $\boldsymbol{k}$ space, as can be

found in the literature.[21,22,27] This is no surprise since these two quantities are directly proportional, as derived in Sec. II D 2, Eq. (15).

From the mathematical point of view, Eq. (23) is an eigenvector-eigenvalue problem that can be solved by means of linear algebra. A detailed analysis of such a problem reveals[27] that for a given value of $N_{y,\nu}^{(\omega)}$ (we recall that $N_{x,\nu}^{(\omega)}$ is assumed to be zero) there exist four independent solutions, i.e., four different eigenvectors $\boldsymbol{\mathcal{E}}_{\nu,p,d}^{(\omega)}$ and their corresponding eigenvalues $(N_{\nu,p,d}^{(\omega)})^2$. The two pairs of these solutions are characterized by the opposite values of the z component of the normalized wave vector $\boldsymbol{N}_{\nu,p,d}^{(\omega)}$. This is the reason for the introduction of the direction index $d=\pm$, where $d=+$ and $d=-$ correspond to the light propagating in the positive $(N_{z,\nu,p,+}^{(\omega)}>0)$ and negative $(N_{z,\nu,p,-}^{(\omega)}<0)$ z directions, respectively. Furthermore, the two eigenvectors corresponding to a given pair characterized by the same value of d are orthogonal, i.e., corresponding to two orthogonal polarization states of the field. This is the reason for the introduction of the polarization index p.

When the form of the permittivity tensor $\epsilon_{ij,\nu}^{(\omega)}$ is general, the solution of the wave equation (23) leads to finding the roots of the fourth degree polynomial. In this case, an analytical solution is very complicated and thus the solution is determined numerically. For the purpose of clarity in the subsequent derivations, we maintain the p and d indices and denote the eigenvectors as $\boldsymbol{\mathcal{E}}_{\nu,p,d}^{(\omega)}$ and the corresponding eigenvalues as $(N_{\nu,p,d}^{(\omega)})^2$.

2. Field distribution across the νth layer

As follows from Eq. (6), the field in the $\boldsymbol{r}$ space within any layer of the multilayer system can be expressed as a sum (integral) of modes in the $\boldsymbol{q}$ space. However, we will look in more detail at one single mode characterized by a particular value of $\boldsymbol{q}$. To be more precise, due to the normalization introduced above and the choice of the coordinate system $(N_{x,\nu}^{(\omega)}=0)$, we will deal in the following analysis with a mode characterized by a particular value of $N_{y,\nu}^{(\omega)}$, i.e., $\boldsymbol{q}=k_0^{(\omega)}[0,N_{y,\nu}^{(\omega)}]$.

The electric field in the νth layer corresponding to such a mode can be written as

$$\boldsymbol{E}_{\nu}^{(\omega)}(y,z)=\sum_{p=1,2}\sum_{d=\pm}\mathcal{E}_{\nu,p,d}^{(\omega)}\hat{\boldsymbol{e}}_{\nu,p,d}^{(\omega)}\times\exp[ik_0^{(\omega)}(N_{y,\nu}^{(\omega)}y+N_{z,\nu,p,d}^{(\omega)}(z-z_\nu))], \tag{24}$$

where $N_{z,\nu,p,d}^{(\omega)}=\sqrt{(N_{\nu,p,d}^{(\omega)})^2-(N_{y,\nu}^{(\omega)})^2}$, and $(N_{\nu,p,d}^{(\omega)})^2$ is the eigenvalue corresponding to the eigenvector $\boldsymbol{\mathcal{E}}_{\nu,p,d}^{(\omega)}$, as mentioned earlier. In order to describe the field distribution in the superstrate (layer $\nu=0$) correctly, $z_0=z_1$ has to be considered in Eq. (24).

The expression for the magnetic field in the νth layer can be derived from the Maxwell equation (3b) using the expression (24) for the electric field. After some simple algebraic manipulation, one arrives at the formula

$$\boldsymbol{H}_{\nu}^{(\omega)}(y,z)=\sum_{p=1,2}\sum_{d=\pm}\mathcal{H}_{\nu,p,d}^{(\omega)}\hat{\boldsymbol{h}}_{\nu,p,d}^{(\omega)}\times\exp[ik_0^{(\omega)}(N_{y,\nu}^{(\omega)}y+N_{z,\nu,p,d}^{(\omega)}(z-z_\nu))], \tag{25}$$

where $\mathcal{H}_{\nu,p,d}^{(\omega)}=(N_{\nu,p,d}^{(\omega)}/\eta_0)\mathcal{E}_{\nu,p,d}^{(\omega)}$ and $\hat{\boldsymbol{h}}_{\nu,p,d}^{(\omega)}=(\boldsymbol{N}_{\nu,p,d}^{(\omega)}\times\hat{\boldsymbol{e}}_{\nu,p,d}^{(\omega)})/N_{\nu,p,d}^{(\omega)}$, in which $\eta_0=\sqrt{\mu_0/\epsilon_0}$ is the vacuum impedance.

3. Boundary conditions and the matrix formalism

To obtain the profile of the fundamental EM field throughout the entire multilayer structure, the boundary conditions have to be applied. They can be derived from the Maxwell equations (3), as shown in the textbooks on electromagnetism.[21,22,29] In the absence of surface charges and currents, the boundary conditions require that the tangential (i.e., x and y) components of the electric and magnetic fields be continuous at each interface. When expressions (24) and (25) are considered, the boundary conditions at the $(\nu+1)$th interface can be written in a compact matrix form as[26,27,30]

$$D_{\nu}^{(\omega)}P_{\nu}^{(\omega)}\boldsymbol{A}_{\nu}^{(\omega)}=\begin{bmatrix}E_{x,\nu+1-\epsilon}^{(\omega)}\\ \eta_0H_{y,\nu+1-\epsilon}^{(\omega)}\\ E_{y,\nu+1-\epsilon}^{(\omega)}\\ \eta_0H_{x,\nu+1-\epsilon}^{(\omega)}\end{bmatrix}=\begin{bmatrix}E_{x,\nu+1+\epsilon}^{(\omega)}\\ \eta_0H_{y,\nu+1+\epsilon}^{(\omega)}\\ E_{y,\nu+1+\epsilon}^{(\omega)}\\ \eta_0H_{x,\nu+1+\epsilon}^{(\omega)}\end{bmatrix}=D_{\nu+1}^{(\omega)}\boldsymbol{A}_{\nu+1}^{(\omega)},\quad \nu=1,\ldots,M+1, \tag{26}$$

where $\eta_0=\sqrt{\mu_0/\epsilon_0}$ is the vacuum impedance. The quantities $E_{a,\nu+1\pm\epsilon}$ and $H_{a,\nu+1\pm\epsilon}$, where $a=x,y$ and $\epsilon\to0$, are the x and y components of the electric and magnetic fields just under (subscript $\nu+1+\epsilon$) and above (subscript $\nu+1-\epsilon$) the $(\nu+1)$th interface. The matrices $D_{\nu}^{(\omega)}$ and $P_{\nu}^{(\omega)}$ are, respectively, the dynamic and propagation matrices given by

$$D_{\nu}^{(\omega)}=\begin{pmatrix}\hat{\boldsymbol{e}}_{\nu,1,+}^{(\omega)}\cdot\hat{\boldsymbol{x}} & \hat{\boldsymbol{e}}_{\nu,1,-}^{(\omega)}\cdot\hat{\boldsymbol{x}} & \hat{\boldsymbol{e}}_{\nu,2,+}^{(\omega)}\cdot\hat{\boldsymbol{x}} & \hat{\boldsymbol{e}}_{\nu,2,-}^{(\omega)}\cdot\hat{\boldsymbol{x}}\\ N_{\nu,1,+}^{(\omega)}\hat{\boldsymbol{h}}_{\nu,1,+}^{(\omega)}\cdot\hat{\boldsymbol{y}} & N_{\nu,1,-}^{(\omega)}\hat{\boldsymbol{h}}_{\nu,1,-}^{(\omega)}\cdot\hat{\boldsymbol{y}} & N_{\nu,2,+}^{(\omega)}\hat{\boldsymbol{h}}_{\nu,2,+}^{(\omega)}\cdot\hat{\boldsymbol{y}} & N_{\nu,2,-}^{(\omega)}\hat{\boldsymbol{h}}_{\nu,2,-}^{(\omega)}\cdot\hat{\boldsymbol{y}}\\ \hat{\boldsymbol{e}}_{\nu,1,+}^{(\omega)}\cdot\hat{\boldsymbol{y}} & \hat{\boldsymbol{e}}_{\nu,1,-}^{(\omega)}\cdot\hat{\boldsymbol{y}} & \hat{\boldsymbol{e}}_{\nu,2,+}^{(\omega)}\cdot\hat{\boldsymbol{y}} & \hat{\boldsymbol{e}}_{\nu,2,-}^{(\omega)}\cdot\hat{\boldsymbol{y}}\\ N_{\nu,1,+}^{(\omega)}\hat{\boldsymbol{h}}_{\nu,1,+}^{(\omega)}\cdot\hat{\boldsymbol{x}} & N_{\nu,1,-}^{(\omega)}\hat{\boldsymbol{h}}_{\nu,1,-}^{(\omega)}\cdot\hat{\boldsymbol{x}} & N_{\nu,2,+}^{(\omega)}\hat{\boldsymbol{h}}_{\nu,2,-}^{(\omega)}\cdot\hat{\boldsymbol{x}} & N_{\nu,2,-}^{(\omega)}\hat{\boldsymbol{h}}_{\nu,2,-}^{(\omega)}\cdot\hat{\boldsymbol{x}}\end{pmatrix} \tag{27}$$

and

$$P_{\nu}^{(\omega)}=\begin{pmatrix} \exp[ik_0^{(\omega)}N_{z,\nu,1,+}^{(\omega)}t_\nu] & 0 & 0 & 0 \\ 0 & \exp[ik_0^{(\omega)}N_{z,\nu,1,-}^{(\omega)}t_\nu] & 0 & 0 \\ 0 & 0 & \exp[ik_0^{(\omega)}N_{z,\nu,2,+}^{(\omega)}t_\nu] & 0 \\ 0 & 0 & 0 & \exp[ik_0^{(\omega)}N_{z,\nu,2,-}^{(\omega)}t_\nu] \end{pmatrix}. \tag{28}$$

The vector $\boldsymbol{A}_{\nu}^{(\omega)}$ in Eq. (26) is defined using the modal magnitudes $\mathcal{E}_{\nu,p,d}^{(\omega)}$ as

$$\boldsymbol{A}_{\nu}^{(\omega)}\equiv[\mathcal{E}_{\nu,1,+}^{(\omega)},\mathcal{E}_{\nu,1,-}^{(\omega)},\mathcal{E}_{\nu,2,+}^{(\omega)},\mathcal{E}_{\nu,2,-}^{(\omega)}]^{\mathrm{T}}, \tag{29}$$

where $\boldsymbol{x}^{\mathrm{T}}$ denotes the transposition of the vector $\boldsymbol{x}$. It denotes the vector of the modal magnitudes inside the νth layer in the vicinity of the νth interface, as depicted in Fig. 3.

In the derivation of Eq. (26), the relation $N_{y,0}^{(\omega)}=N_{y,1}^{(\omega)}=\cdots=N_{y,M+1}^{(\omega)}$ was considered. This corresponds to the well-known Snell's law on the conservation of the tangential component of the wave vector across the multilayer structure. Because of this relation, all $N_{y,\nu}^{(\omega)}$'s will be denoted by a single variable $N_y^{(\omega)}$. This step is important since it binds the modes of the different layers of the multilayer structure into a single mode of the *entire* multilayer system, which is parametrized by a single parameter $N_y^{(\omega)}$.

As mentioned above, the wave equation (23) has four solutions which cannot be, in general, expressed in a simple analytical way. However, for an isotropic nonmagnetic medium characterized by a permittivity tensor in a diagonal form $\epsilon_{ij,\nu}^{(\omega)}\equiv\epsilon_{\nu}^{(\omega)}\delta_{ij}$, where δ_{ij} is the Kronecker δ symbol, the solutions can be found easily. One possible set of solutions corresponds to two pairs of **s**- (TE) and **p**- (TM) polarized modes, one propagating in the positive and the other in the negative z directions. Due to this interpretation, the index p denoting the polarization state of the modes can be considered to take values $p=\mathbf{s},\mathbf{p}$, as opposed to $p=1,2$ considered in the previous, more general case. The magnitude of the normalized wave vector is equal to $N_{\nu,p,d}=N_{\nu}^{(\omega)}=\sqrt{\epsilon_{\nu}^{(\omega)}}$ for all combinations of indices p and d, and the corresponding z component is evaluated as

$$N_{z,\nu,\mathbf{s},\pm}^{(\omega)}=N_{z,\nu,\mathbf{p},\pm}^{(\omega)}=N_{z,\nu,\pm}^{(\omega)}\equiv\pm N_{z,\nu}^{(\omega)}\equiv\pm\sqrt{\epsilon_{\nu}^{(\omega)}-(N_y^{(\omega)})^2} \tag{30}$$

for the modes propagating in the positive $(+)$ and negative $(-)$ z directions.

The vector modal amplitudes can be written in the forms

$$\boldsymbol{\mathcal{E}}_{\nu,\mathbf{s},\pm}^{(\omega)}=\mathcal{E}_{\nu,\mathbf{s},\pm}^{(\omega)}\hat{\boldsymbol{e}}_{\nu,\mathbf{s},\pm}^{(\omega)},\quad \boldsymbol{\mathcal{E}}_{\nu,\mathbf{p},\pm}^{(\omega)}=\mathcal{E}_{\nu,\mathbf{p},\pm}^{(\omega)}\hat{\boldsymbol{e}}_{\nu,\mathbf{p},\pm}^{(\omega)}, \tag{31}$$

where the respective unity vectors characterizing the **s** and **p** polarization directions are given by

$$\hat{\boldsymbol{e}}_{\nu,\mathbf{s},\pm}^{(\omega)}=[1,0,0],$$

$$\hat{\boldsymbol{e}}_{\nu,\mathbf{p},\pm}^{(\omega)}=[0,N_{z,\nu,\pm}^{(\omega)},-N_y^{(\omega)}]/N_{\nu}^{(\omega)}. \tag{32}$$

Combining Eqs. (31) and (32), the dynamic and propagation matrices (27) and (28) for the isotropic nonmagnetic medium can be written as

$$D_{\nu}^{(\omega)}=\begin{pmatrix} 1 & 1 & 0 & 0 \\ N_{z,\nu,+}^{(\omega)} & N_{z,\nu,-}^{(\omega)} & 0 & 0 \\ 0 & 0 & N_{z,\nu,+}^{(\omega)}/N_{\nu}^{(\omega)} & N_{z,\nu,-}^{(\omega)}/N_{\nu}^{(\omega)} \\ 0 & 0 & -N_{\nu}^{(\omega)} & -N_{\nu}^{(\omega)} \end{pmatrix}, \tag{33}$$

and

$$P_{\nu}^{(\omega)}=\begin{pmatrix} \exp[ik_0^{(\omega)}N_{z,\nu,+}^{(\omega)}t_\nu] & 0 & 0 & 0 \\ 0 & \exp[ik_0^{(\omega)}N_{z,\nu,-}^{(\omega)}t_\nu] & 0 & 0 \\ 0 & 0 & \exp[ik_0^{(\omega)}N_{z,\nu,+}^{(\omega)}t_\nu] & 0 \\ 0 & 0 & 0 & \exp[ik_0^{(\omega)}N_{z,\nu,-}^{(\omega)}t_\nu] \end{pmatrix}. \tag{34}$$

Furthermore, the vector $\boldsymbol{A}_{\nu}^{(\omega)}$, whose general form is defined in Eq. (29), can be written as

$$\boldsymbol{A}_{\nu}^{(\omega)}\equiv[\mathcal{E}_{\nu,\mathbf{s},+}^{(\omega)},\mathcal{E}_{\nu,\mathbf{s},-}^{(\omega)},\mathcal{E}_{\nu,\mathbf{p},+}^{(\omega)},\mathcal{E}_{\nu,\mathbf{p},-}^{(\omega)}]^{\mathrm{T}}. \tag{35}$$

As mentioned earlier, a typical configuration of the SHG experiments involves a fundamental beam interrogating the multilayer system, and the SHG field which is observed in either the superstrate or the substrate [see Fig. 2(a)]. In the majority of cases, both the superstrate and the substrate consist of isotropic and nonmagnetic materials. Consequently, the field in those media can be decomposed into the **s**- and **p**-polarized modes.

Typically, the fundamental beam impinges on the sample at a defined incident angle $\theta_0^{(\omega)}$. This determines the value of $N_y^{(\omega)}$, which is conserved across the multilayer system, to be

given by

$$N_y^{(\omega)} = \sqrt{\epsilon_0^{(\omega)}} \sin\theta_0^{(\omega)} = \sqrt{\epsilon_{M+1}^{(\omega)}} \sin\theta_{M+1}^{(\omega)}. \tag{36}$$

Furthermore, $\mathcal{E}_{0,\mathbf{s},+}^{(\omega)}$ and $\mathcal{E}_{0,\mathbf{p},+}^{(\omega)}$, representing the magnitudes of the **s**- and **p**-polarized components of the incident beam, can be considered as given parameters.

To derive the expression relating the modal amplitudes of the field in the substrate and the νth layer, one has to recursively apply Eq. (26). This procedure results in the expression

$$\boldsymbol{A}_0^{(\omega)} = L_\nu^{(\omega)} \boldsymbol{A}_\nu^{(\omega)}, \tag{37}$$

where the matrix $L_\nu^{(\omega)}$ can be calculated from the definition

$$L_\nu^{(\omega)} \equiv [D_0^{(\omega)}]^{-1} D_1^{(\omega)} [P_1^{(\omega)}]^{-1} \cdots D_{\nu-1}^{(\omega)} [P_{\nu-1}^{(\omega)}]^{-1} \times [D_{\nu-1}^{(\omega)}]^{-1} D_\nu^{(\omega)}. \tag{38}$$

In this definition, $L_0^{(\omega)} \equiv 1$ is considered. The relation between the modal amplitudes of the field in the superstrate and substrate can subsequently be written as

$$\boldsymbol{A}_0^{(\omega)} = L_{M+1}^{(\omega)} \boldsymbol{A}_{M+1}^{(\omega)}. \tag{39}$$

Due to the fact that there is no light incident from the substrate side of the sample [see Fig. 2(a)], the modal magnitudes $\mathcal{E}_{M+1,\mathbf{s},-}^{(\omega)}$ and $\mathcal{E}_{M+1,\mathbf{p},-}^{(\omega)}$ are identically equal to zero. Consequently, the modal amplitudes of the transmitted field $\mathcal{E}_{M+1,\mathbf{s},+}^{(\omega)}$ and $\mathcal{E}_{M+1,\mathbf{p},+}^{(\omega)}$ can be calculated from Eq. (39), in which $\boldsymbol{A}_0^{(\omega)}$ is given by Eq. (35) with $\nu = 0$. Subsequently, the vector $\boldsymbol{A}_{M+1}^{(\omega)}$ is evaluated as

$$\boldsymbol{A}_{M+1}^{(\omega)} = [\mathcal{E}_{M+1,\mathbf{s},+}^{(\omega)}, 0, \mathcal{E}_{M+1,\mathbf{p},+}^{(\omega)}, 0]^{\mathrm{T}}. \tag{40}$$

After some simple algebraic manipulations, one can derive the expression between the transmitted and incident field magnitudes in the explicit form

$$\begin{bmatrix} \mathcal{E}_{M+1,\mathbf{s},+}^{(\omega)} \\ \mathcal{E}_{M+1,\mathbf{p},+}^{(\omega)} \end{bmatrix} = \begin{pmatrix} L_{11,M+1}^{(\omega)} & L_{13,M+1}^{(\omega)} \\ L_{31,M+1}^{(\omega)} & L_{33,M+1}^{(\omega)} \end{pmatrix}^{-1} \begin{bmatrix} \mathcal{E}_{0,\mathbf{s},+}^{(\omega)} \\ \mathcal{E}_{0,\mathbf{p},+}^{(\omega)} \end{bmatrix}. \tag{41}$$

Having calculated the components of the vector $\boldsymbol{A}_{M+1}^{(\omega)}$ from Eq. (41), one can evaluate the magnitudes $\mathcal{E}_{\nu,p,d}^{(\omega)}$ for each of the layers $\nu = 1, \ldots, M$ by simply substituting the corresponding $\boldsymbol{A}_\nu^{(\omega)}$ defined in Eq. (29) into Eqs. (37) and (39), i.e., from the expression

$$\boldsymbol{A}_\nu^{(\omega)} = (L_\nu^{(\omega)})^{-1} L_{M+1}^{(\omega)} \boldsymbol{A}_{M+1}^{(\omega)}. \tag{42}$$

In the following section, the fundamental field *at* the layer interface will be required for the calculation of the point dipole. To derive explicit formulas for the field at the νth interface, we use expression (24). For the particular value of $N_y^{(\omega)}$, the components of the vectors $\hat{\boldsymbol{e}}_{\nu,p,d}^{(\omega)}$ are calculated from the wave equation (23), and the magnitudes $\mathcal{E}_{\nu,p,d}^{(\omega)}$ forming the vector $\boldsymbol{A}_\nu^{(\omega)}$ are evaluated from Eq. (42).

In the process of evaluation of the field at the layer interface, the x and y components of the fundamental field do not impose any problem as they are continuous across the interface. On the other hand, the problem arises as to which value of the field's z component should be used, since the z component is not continuous across the layer interface. In principle, there has been two approaches to this problem used in the literature.[1,31,32] In one of them, the value of the z component of the field at the interface is taken as the average of the values immediately below and above the interface. Employing the formalism developed above, this approach leads to the expression for the total field at the νth interface corresponding to the mode characterized by $N_y^{(\omega)}$ in the form

$$\begin{aligned} \boldsymbol{E}_{\nu,\mathrm{int}}^{(\omega)}(y, z_\nu) &\equiv \frac{1}{2}[\boldsymbol{E}_{\nu-\epsilon}^{(\omega)}(y, z_\nu - \epsilon) + \boldsymbol{E}_{\nu+\epsilon}^{(\omega)}(y, z_\nu + \epsilon)] \\ &= \frac{1}{2} \sum_{p=1,2} \sum_{d=\pm} (\mathcal{E}_{\nu-1,p,d}^{(\omega)} \hat{\boldsymbol{e}}_{\nu-1,p,d}^{(\omega)} \\ &\quad \times \exp[i k_0^{(\omega)} N_{z,\nu-1,p,d}^{(\omega)} t_{\nu-1}] \\ &\quad + \mathcal{E}_{\nu,p,d}^{(\omega)} \hat{\boldsymbol{e}}_{\nu,p,d}^{(\omega)}) \exp[i k_0^{(\omega)} N_y^{(\omega)} y], \end{aligned} \tag{43}$$

where the subscripts $\nu + \epsilon$ and $\nu - \epsilon$ correspond to the electric field expressed just under and above the νth interface, respectively.

In the other approach, an infinitesimally thin vacuum layer is inserted in place of the interface and the z component of the field at the interface is taken simply as the z component of the field in this vacuum layer. Using this approach, the total field at the νth interface corresponding to the mode, characterized by $N_y^{(\omega)}$, can be written as

$$\boldsymbol{E}_{\nu,\mathrm{int}}^{(\omega)}(y, z_\nu) = \sum_{p=\mathbf{s},\mathbf{p}} \sum_{d=\pm} (\mathcal{E}_{\mathrm{vac},\nu,p,d}^{(\omega)} \hat{\boldsymbol{e}}_{\mathrm{vac},p,d}^{(\omega)}) \exp[i k_0^{(\omega)} N_y^{(\omega)} y]. \tag{44}$$

The magnitudes $\mathcal{E}_{\mathrm{vac},\nu,p,d}^{(\omega)}$ comprise the vector $\boldsymbol{A}_{\mathrm{vac},\nu}^{(\omega)} \equiv [\mathcal{E}_{\mathrm{vac},\nu,\mathbf{s},+}^{(\omega)}, \mathcal{E}_{\mathrm{vac},\nu,\mathbf{s},-}^{(\omega)}, \mathcal{E}_{\mathrm{vac},\nu,\mathbf{p},+}^{(\omega)}, \mathcal{E}_{\mathrm{vac},\nu,\mathbf{p},-}^{(\omega)}]^{\mathrm{T}}$ which can be obtained from

$$\boldsymbol{A}_{\mathrm{vac},\nu}^{(\omega)} = [D_{\mathrm{vac}}^{(\omega)}]^{-1} D_\nu^{(\omega)} \boldsymbol{A}_\nu^{(\omega)}. \tag{45}$$

In this expression, the matrix $D_{\mathrm{vac}}^{(\omega)}$ is given by Eq. (33), in which substitutions $N_{\mathrm{vac}}^{(\omega)} = 1$ and $N_{z,\mathrm{vac},\pm}^{(\omega)} = \pm\sqrt{1 - (N_y^{(\omega)})^2}$ are applied. The components of the vectors $\hat{\boldsymbol{e}}_{\mathrm{vac},p,d}^{(\omega)}$ are calculated from Eq. (32) where the same substitutions are applied. The matrix product preceding the vector $\boldsymbol{A}_\nu^{(\omega)}$ in Eq. (45) represents the transmission of the field from the νth layer to the vacuum layer inserted in place of the νth interface.

In summary of this section, we derived explicit formulas for the fundamental electric field at each interface of the multilayer system. The field can be expressed as a sum of the plane electromagnetic waves (modes), each characterized by $N_y^{(\omega)}$. For a particular mode, i.e., for a given value of $N_y^{(\omega)}$, the field at the νth interface (i.e., at $z = z_\nu$) can be formally written as

$$\boldsymbol{E}_{\nu,\mathrm{int}}^{(\omega)}(y, z_\nu) \equiv \tilde{\boldsymbol{E}}_{\nu,\mathrm{int}}^{(\omega)}(N_y^{(\omega)}) \exp[i k_0^{(\omega)} N_y^{(\omega)} y], \tag{46}$$

as follows from expressions (43) and (44). In this equation, $\tilde{\boldsymbol{E}}^{(\omega)}_{\nu,\mathrm{int}}(N^{(\omega)}_{y})$ denotes the vector *amplitude* of the fundamental field at the νth interface at $y=0$, while the exponential term determines the distribution of the *phase* at the interface. The amplitude is defined either in Eq. (43) or (44), depending on which approach to the choice of the field's z component is opted for.

In the numerical calculations, we use the approach based on Eq. (43) to calculate the electric field at the interface. This is because the profile of the permittivity tensor $\boldsymbol{\epsilon}$ in *real* structures is not steplike (as in an idealized stratified structure), but is continuous across the interface. As a consequence, the electrical field across the interface is continuous as well and thus the field *at* the interface can be assumed to be an average of the values immediately above and below the interface. On the other hand, using the second approach together with the renormalization of some tensor elements $\chi_{ijk,\nu}$ would lead to the same point dipole amplitude $\boldsymbol{\mu}^{(2\omega)}_{\nu}$ and thus to the same radiated intensity. In this sense, therefore, the two approaches are interchangeable.

F. Second-harmonic field generated by a single point dipole

As mentioned in the introductory section, the SH field is assumed to be generated *at* the interfaces of the layers comprising the multilayer system, as a consequence of microscopic symmetry breaking. In the context of the formalism employed in this paper this means that the point electric dipoles, which act as sources of the SH field, are assumed to be located at the layer interfaces.

Before we can proceed with some general distribution of point dipoles across the interfaces, it is necessary to describe the SH radiation produced by a *single* point dipole. This is done using the following assumptions.

(i) An infinitesimally thin layer of isotropic and lossless dielectric material characterized by scalar permittivity $\overline{\boldsymbol{\epsilon}}^{(\omega_0)}_{\nu}$ is inserted in place of the dipole location, i.e., at the νth interface, and the location of the oscillating dipole is kept inside this layer, as shown in Fig. 3. The value of $\overline{\boldsymbol{\epsilon}}^{(\omega_0)}_{\nu}$ is unknown, however, we will assume that the layer is comprised of vacuum, i.e., $\overline{\boldsymbol{\epsilon}}^{(\omega_0)}_{\nu}=1$.[1,33] The choice of this specific value does not prevent the calculations to be general. This can be understood by realizing that the relation between the fundamental and radiated (SH) fields, which is affected by the value of $\overline{\boldsymbol{\epsilon}}^{(\omega_0)}_{\nu}$, also depends on the values of the nonlinear susceptibility tensor χ_{ν}. Hence, the same relationship between the fundamental and radiated (SH) fields can be obtained for any value of $\overline{\boldsymbol{\epsilon}}^{(\omega_0)}_{\nu}$ by renormalizing the elements of the tensor χ_{ν}.[33]

(ii) The radiating dipole, namely, its complex vector amplitude and the frequency of oscillations, is not affected by the radiation generated by this dipole or by the radiation generated by any other of the radiating dipoles. In other words, we assume that Eq. (2) is valid independently for every dipole located at any position on the interface, with the vector of the electric field being expressed at the dipole position.

Assumption (i) allows us to deal *separately* with the two main problems imposed by the presence of the point dipole at the interface. In particular, it allows us to deal first with the influence of the point dipole on the boundary conditions *at* the dipole location inside the ultrathin layer, i.e., at the location with no interface, and then to analyze the boundary conditions at the interfaces between the ultrathin layer and the layers surrounding the dipole. These steps will effectively lead to a description of radiation produced by a dipole located at an interface. Assumption (ii) allows us to directly combine the fields produced by each individual dipole and evaluate the grand total SH field produced by the entire multilayer structure.

1. Definition of the source of the SH field

As mentioned above, the SH field is assumed to be generated by a point electric dipole oscillating at frequency 2ω. To enable the use of some previously mentioned equations, we denote this frequency as ω_0, keeping in mind that $\omega_0=2\omega$ whenever it appears in the context of the SH field. The dipole is assumed to be located at $\boldsymbol{r}_{\nu}=[x_{\nu},y_{\nu},z_{\nu}]$, which will later on correspond to a location at the νth interface.

In Maxwell equations (3), it is the current density $\boldsymbol{j}^{(\omega_0)}$ and the charge density $\rho^{(\omega_0)}$ that act as the source of the EM field. The current density is obtained as the time derivative of the electric dipole density $\boldsymbol{\mu}(\boldsymbol{r},t)=\boldsymbol{\mu}^{(\omega_0)}_{\nu}\delta(\boldsymbol{r}-\boldsymbol{r}_{\nu})\exp[-i\omega_0 t]$ and can be written as $\boldsymbol{j}(\boldsymbol{r},t)\equiv\partial\boldsymbol{\mu}(\boldsymbol{r},t)/\partial t=\boldsymbol{j}^{(\omega_0)}\exp[-i\omega_0 t]$, where[21,22]

$$\boldsymbol{j}^{(\omega_0)}=-i\omega_0\boldsymbol{\mu}^{(\omega_0)}_{\nu}\delta(\boldsymbol{r}-\boldsymbol{r}_{\nu}). \tag{47}$$

In this equation, the complex amplitude $\boldsymbol{\mu}^{(\omega_0)}_{\nu}$ of the dipole is given by Eq. (2), where the fundamental field is calculated from Eq. (46).

With regard to the charge density $\rho^{(\omega_0)}$, we assume for a moment that the point dipole is parallel to the z axis and is not oscillating. Such a dipole consists of a positive and a negative point charge, denoted as Q and $-Q$, located at $z=z_{\nu}-\boldsymbol{\epsilon}$ and $z=z_{\nu}+\boldsymbol{\epsilon}$, respectively. The charge density corresponding to such a charge constellation can be formally expressed as

$$\rho=Q\delta(x-x_{\nu})\delta(y-y_{\nu})\lim_{\boldsymbol{\epsilon}\to 0}[\delta(z-(z_{\nu}-\boldsymbol{\epsilon}))-\delta(z-(z_{\nu}+\boldsymbol{\epsilon}))]. \tag{48}$$

Since the dipole strength is equal to $\mu_z=2Q\boldsymbol{\epsilon}$, a simple modification of Eq. (48) leads to the expression

$$\rho=-\mu_z\delta(x-x_{\nu})\delta(y-y_{\nu})\frac{\partial}{\partial z}\delta(z-z_{\nu}). \tag{49}$$

Considering a general orientation of the point dipole and the fact that it oscillates, the above expression for the charge density can be generalized to $\rho(\boldsymbol{r},t)=\rho^{(\omega_0)}\exp[-i\omega_0 t]$, where

$$\rho^{(\omega_0)}=-\boldsymbol{\mu}^{(\omega_0)}_{\nu}\cdot\nabla\delta(\boldsymbol{r}-\boldsymbol{r}_{\nu}). \tag{50}$$

In this equation, $\nabla\delta$ denotes the gradient of the δ function.

2. Boundary conditions in the presence of an electric point dipole

In this section, we analyze the influence of an oscillating dipole on the normal and transversal components of the field vectors. Although a similar analysis was reported in the literature[34], it cannot directly be used here since the authors dealt with the conditions around a homogeneous and infinitesimally thin polarization *sheet* rather than a point dipole. Nevertheless, the formalism developed there can advantageously be applied in our analysis.

Initially, we carry out the analysis in the $\boldsymbol{r}$ space. The expressions will subsequently be transformed into the $\boldsymbol{q}$ space where they can be directly incorporated into the matrix formalism describing the propagation of light in the multilayer structure.

Let us consider a function f which contains discontinuities and singularities of the type of the Dirac δ function or its derivatives at a location generally denoted as $x_{i,\nu}$, where x_1, x_2, and x_3 correspond to x, y, and z coordinates, respectively. Such a function can be written in the form

$$f(x_i)=\{f\}+\Delta f\,\vartheta(x_i-x_{i,\nu})+f_\delta\,\frac{1}{k_0^u}\,\delta(x_i-x_{i,\nu})+\cdots. \tag{51}$$

Employing a well-known treatment of such a function,[34,35] its derivative can be written as

$$\frac{\partial f}{\partial x_i}=\left\{\frac{\partial f}{\partial x_i}\right\}+[f(x_{i,\nu+\epsilon})-f(x_{i,\nu-\epsilon})]\,\delta(x_i-x_{i,\nu})+f_\delta\,\frac{1}{k_0^u}\,\frac{\partial}{\partial x_i}\,\delta(x_i-x_{i,\nu})+\cdots, \tag{52}$$

where $\{\partial f/\partial x_i\}$ denotes the derivative of the function almost everywhere and $f(x_{i,\nu\pm\epsilon})$ is the value of the function at $x_i=x_{i,\nu}\pm\epsilon$, $\epsilon\to 0$. The factor $1/k_0^u$ in Eqs. (51) and (52) was added in order to ensure that $f(x)$ and f_δ have the same units.

In the context of the following analysis, the function f can be any of the components of the field vectors. Equation (52) has an important implication: Since the sources of the SH field in the Maxwell equations (3) contain singularities of the type of the Dirac δ function and its derivatives, as shown in Eqs. (47) and (50), the field vectors must contain discontinuities as well as singularities of the same type.

In the following derivations, we add an overbar above all variables which are related to the electromagnetic waves inside the thin sheet placed at the νth interface, e.g., $\overline{\boldsymbol{\epsilon}}_\nu^{(\omega_0)}$, $\overline{\boldsymbol{N}}_\nu^{(\omega_0)}$, $\hat{\overline{\boldsymbol{e}}}_{\nu,\mathbf{s},\pm}^{(\omega_0)}$, $\hat{\overline{\boldsymbol{e}}}_{\nu,\mathbf{p},\pm}^{(\omega_0)}$, $\overline{\boldsymbol{D}}$, $\overline{\boldsymbol{\mathcal{D}}}$, etc., in order to distinguish between the variables inside the thin sheet located at the νth interface and those inside the νth layer.

(a) *Boundary conditions for* $\overline{\boldsymbol{D}}$. Considering the expression (50) for the charge density, the Maxwell equation (3a) can be expressed as[36]

$$\nabla\cdot\overline{\boldsymbol{D}}=\{\nabla\cdot\overline{\boldsymbol{D}}\}+\overline{F}_D(x-x_\nu,y-y_\nu)+(\overline{D}_{z,\nu+\epsilon}-\overline{D}_{z,\nu-\epsilon})\times\delta(z-z_\nu)+\overline{D}_{z,\delta}\frac{1}{k_0^u}\frac{\partial}{\partial z}\delta(z-z_\nu)+\overline{G}_D(z-z_\nu)$$
$$=-\boldsymbol{\mu}_\nu^{(\omega_0)}\cdot\nabla\,\delta(\boldsymbol{r}-\boldsymbol{r}_\nu), \tag{53}$$

where $\overline{G}_D(z-z_\nu)$ containes higher order terms proportional to $\partial^n\delta(z-z_\nu)/\partial z^n$, $n>1$, which are not explicitly spelled out. In this equation, $\overline{F}_D(x-x_\nu,y-y_\nu)$ denotes the terms containing the discontinuities and singularities of the type of the Dirac δ function and its derivatives in the x and y dimensions located at the point dipole position, i.e., at $\boldsymbol{r}=\boldsymbol{r}_\nu$. Since these terms do not contribute to the boundary conditions in the $\boldsymbol{q}$ space, as already discussed in Sec. II D 3, the explicit form of this function can be omitted in the following calculations.

Comparing the terms with the same order of the derivatives of $\delta(z-z_\nu)$, the boundary conditions for the vector $\overline{\boldsymbol{D}}$ in the $\boldsymbol{r}$ space can be written as

$$\{\nabla\cdot\overline{\boldsymbol{D}}\}=0,$$
$$\overline{D}_{z,\nu+\epsilon}-\overline{D}_{z,\nu-\epsilon}=-\mu_{x,\nu}^{(\omega_0)}\,\delta(y-y_\nu)\frac{\partial\delta(x-x_\nu)}{\partial x}-\mu_{y,\nu}^{(\omega_0)}\,\delta(x-x_\nu)\frac{\partial\delta(y-y_\nu)}{\partial y}, \tag{54}$$
$$\overline{D}_{z,\delta}=-\mu_{z,\nu}^{(\omega_0)}k_0^u\,\delta(x-x_\nu)\,\delta(y-y_\nu).$$

The first equation implies the continuity of the normal component of the vector $\overline{\boldsymbol{D}}$ everywhere except at the location of the point dipole.[21,22] This is equivalent to the well-known boundary condition for the medium containing no free charges. The influence of the point dipole is described by the second and third equations. In particular, the discontinuity of the z component of the field $\overline{\boldsymbol{D}}$ at the location of the point dipole is determined by the right-hand side of the second equation. Furthermore, the z component of the vector $\overline{\boldsymbol{D}}$ contains a singularity which is expressed by the right-hand side of the third equation.

The form of the boundary conditions (54) in the $\boldsymbol{r}$ space is not very convenient for further mathematical treatment due to the presence of the δ function and its derivative. On the other hand, the boundary conditions can be elegantly expressed in the $\boldsymbol{q}$ space. In particular, using the properties of the $\boldsymbol{q}$ space discussed in Sec. II D 3 [see Eqs. (17) and (18)], the second equation in Eq. (54) can be written as

$$\Delta\overline{\mathcal{D}}_{z,\nu,\Sigma,\Sigma}\equiv\overline{\mathcal{D}}_{z,\nu+\epsilon,\Sigma,\Sigma}-\overline{\mathcal{D}}_{z,\nu-\epsilon,\Sigma,\Sigma}=(-i\mu_{x,\nu}^{(\omega_0)}k_x-i\mu_{y,\nu}^{(\omega_0)}k_y)(k_0^u)^2\exp[-i\boldsymbol{q}\cdot\boldsymbol{\rho}_\nu], \tag{55}$$

where the vector $\boldsymbol{\rho}_\nu$ has been defined as $\boldsymbol{\rho}_\nu=[x_\nu,y_\nu]$. This equation provides an explicit expression for the magnitude of the discontinuity of the z component of the vector $\overline{\boldsymbol{\mathcal{D}}}_{\nu,\Sigma,\Sigma}$.

The third equation in Eq. (54) implies that, in addition to the discontinuity at $z=z_\nu$, the z component of the vector $\overline{\boldsymbol{D}}$ contains also a singularity that can be written as

$$\overline{\boldsymbol{D}}_\delta = -\mu_{z,\nu}^{(\omega_0)}\delta(\boldsymbol{r}-\boldsymbol{r}_\nu)\hat{z}. \tag{56}$$

However, as mentioned in the discussion after Eq. (22), such a singularity does not affect boundary condition (55). On the other hand, this singularity will affect the boundary conditions for the fields $\overline{\boldsymbol{\mathcal{E}}}$ and $\overline{\boldsymbol{\mathcal{H}}}$, as will be shown below.

(b) *Boundary conditions for* $\overline{\boldsymbol{B}}$. The boundary condition for the vector $\overline{\boldsymbol{B}}$ can be derived from the Maxwell equation (3c) using an equivalent procedure as for the vector $\overline{\boldsymbol{D}}$. In the $\boldsymbol{r}$ space, the condition can be written as

$$\overline{B}_{z,\nu+\epsilon} - \overline{B}_{z,\nu-\epsilon} = 0. \tag{57}$$

In the $\boldsymbol{q}$ space, the boundary condition takes the form

$$\Delta\overline{\mathcal{B}}_{z,\nu,\Sigma,\Sigma} \equiv \overline{\mathcal{B}}_{z,\nu+\epsilon,\Sigma,\Sigma} - \overline{\mathcal{B}}_{z,\nu-\epsilon,\Sigma,\Sigma} = 0. \tag{58}$$

This expression means that the z component of the vector $\overline{\boldsymbol{\mathcal{B}}}$ is continuous around the position of the point dipole.

(c) *Boundary conditions for* $\overline{\boldsymbol{H}}$. The boundary conditions for the field vector $\overline{\boldsymbol{H}}$ can be derived from the Maxwell equation (3d), where the current density is given by Eq. (47). Assuming that the field distribution contains discontinuities and singularities of the type of the Dirac δ function and its derivatives, the left-hand side of Eq. (3d) can be expressed as

$$\nabla\times\overline{\boldsymbol{H}} = \{\nabla\times\overline{\boldsymbol{H}}\} + \overline{\boldsymbol{F}}_H(x-x_\nu, y-y_\nu)+\begin{bmatrix}\delta(x-x_\nu)\\ \delta(y-y_\nu)\\ \delta(z-z_\nu)\end{bmatrix} \times(\overline{\boldsymbol{H}}_{\nu+\epsilon}-\overline{\boldsymbol{H}}_{\nu-\epsilon}) + \overline{\boldsymbol{G}}_H(z-z_\nu), \tag{59}$$

where $\overline{\boldsymbol{G}}_H(z-z_\nu)$ containes higher order terms proportional to $\partial^n\delta(z-z_\nu)/\partial z^n$, $n\geqslant 1$, which are not explicitly spelled out. In this equation, $\overline{\boldsymbol{F}}_H(x-x_\nu, y-y_\nu)$ denotes the terms containing the discontinuities and singularities of the type of the Dirac δ function and its derivatives in the x and y dimensions located at the point dipole position, i.e., at $\boldsymbol{r}=\boldsymbol{r}_\nu$. Since these terms do not contribute to the boundary conditions in the $\boldsymbol{q}$ space, as already discussed in Sec. II D 3, the explicit form of this function can be omitted in the following calculations.

In the evaluation of the right-hand side of Eq. (3d), the singularity of the z component of the vector $\overline{\boldsymbol{D}}$ given in Eq. (56) has to be taken into account. Comparing the terms with the same order of the derivatives of $\delta(z-z_\nu)$, the boundary conditions for the vector $\overline{\boldsymbol{H}}$ in the $\boldsymbol{r}$ space can be written as

$$\{\nabla\times\overline{\boldsymbol{H}}\} = -i\omega_0\{\overline{\boldsymbol{D}}\},$$

$$\overline{H}_{x,\nu+\epsilon} - \overline{H}_{x,\nu-\epsilon} = -i\omega_0\mu_{y,\nu}^{(\omega_0)}\delta(x-x_\nu)\,\delta(y-y_\nu), \tag{60}$$

$$\overline{H}_{y,\nu+\epsilon} - \overline{H}_{y,\nu-\epsilon} = i\omega_0\mu_{x,\nu}^{(\omega_0)}\delta(x-x_\nu)\,\delta(y-y_\nu).$$

The first equation implies the continuity of the tangential components of the vector $\overline{\boldsymbol{H}}$ everywhere except at the location of the point dipole.[21,22] This is equivalent to the well-known boundary condition for the medium containing no free charge currents. The influence of the point dipole is described by the second and third equations. In particular, the discontinuities of the x and y components of the field $\overline{\boldsymbol{H}}$ at the location of the point dipole are determined by the right-hand sides of the second and third equations, respectively. Due to the fact that the right-hand side of Eq. (3d) does not contain terms proportional to $\partial^n\delta(z-z_\nu)/\partial z^n$, where $n=1,2,\ldots$, the field vector $\overline{\boldsymbol{H}}$ does not contain any singularities of the type of the Dirac δ function or its derivatives at the position of the oscillating point dipole.

When boundary conditions (60) are expressed in the $\boldsymbol{q}$ space, the following equations are found:

$$\Delta\overline{\mathcal{H}}_{x,\nu,\Sigma,\Sigma} \equiv \overline{\mathcal{H}}_{x,\nu+\epsilon,\Sigma,\Sigma} - \overline{\mathcal{H}}_{x,\nu-\epsilon,\Sigma,\Sigma} = -i\omega_0\mu_{y,\nu}^{(\omega_0)}(k_0^u)^2\exp[-i\boldsymbol{q}\cdot\boldsymbol{\rho}_\nu],$$

$$\Delta\overline{\mathcal{H}}_{y,\nu,\Sigma,\Sigma} \equiv \overline{\mathcal{H}}_{y,\nu+\epsilon,\Sigma,\Sigma} - \overline{\mathcal{H}}_{y,\nu-\epsilon,\Sigma,\Sigma} = i\omega_0\mu_{x,\nu}^{(\omega_0)}(k_0^u)^2\exp[-i\boldsymbol{q}\cdot\boldsymbol{\rho}_\nu]. \tag{61}$$

These equations provide explicit expressions for the magnitudes of the discontinuities of the x and y components of the vector $\overline{\boldsymbol{\mathcal{H}}}_{\nu,\Sigma,\Sigma}$.

(d) *Boundary conditions for* $\overline{\boldsymbol{E}}$. The boundary condition for the vector $\overline{\boldsymbol{E}}$ can be derived from the Maxwell equation (3b). However, before the equations are explicitly written, the following comments need to be made. Even though the treatment of the point dipole is done in the microscopic level, the medium surrounding the dipole is considered in the macroscopic level, i.e., described by the dielectric permittivity $\overline{\boldsymbol{\epsilon}}_\nu^{(\omega_0)}$ and the magnetic permeability is in this work assumed to be equal to the vacuum permeability μ_0. This means that the relations between the pairs of the electric and magnetic field vectors take the forms $\overline{\boldsymbol{D}}=\epsilon_0\overline{\boldsymbol{\epsilon}}_\nu^{(\omega_0)}\overline{\boldsymbol{E}}$ and $\overline{\boldsymbol{B}}=\mu_0\overline{\boldsymbol{H}}$, respectively. These equations are valid *everywhere*, i.e., even at the location of the point dipole. The former relation implies that the vector $\overline{\boldsymbol{E}}$ contains a singularity. Since the vector $\overline{\boldsymbol{E}}$ can be written as $\overline{\boldsymbol{E}}=\{\overline{\boldsymbol{E}}\}+\Delta\overline{\boldsymbol{E}}\vartheta(z-z_\nu)+\overline{\boldsymbol{E}}_\delta(k_0^u)^{-1}\delta(z-z_\nu)+\cdots$, as mentioned in Eq. (51), the singularities $\overline{\boldsymbol{E}}_\delta$ and $\overline{\boldsymbol{D}}_\delta$ are related by equality $\overline{\boldsymbol{E}}_\delta=\overline{\boldsymbol{D}}_\delta/(\epsilon_0\overline{\boldsymbol{\epsilon}}_\nu^{(\omega_0)})$, where $\overline{\boldsymbol{D}}_\delta$ is given by Eq. (56). The latter equation implies that since the vector $\overline{\boldsymbol{H}}$ contains no singularities at the dipole position, the vector $\overline{\boldsymbol{B}}$ does not contain any either.

When the above equations are taken into account and substituted into the Maxwell equation (3b), the comparison of the terms with the same order of the derivatives of $\delta(z-z_\nu)$ leads to the following set of equations:

$$\{\nabla\times\bar{\boldsymbol{E}}\}=i\omega_0\{\bar{\boldsymbol{B}}\},$$

$$\bar{E}_{x,\nu+\epsilon}-\bar{E}_{x,\nu-\epsilon}=-\frac{1}{\epsilon_0\bar{\epsilon}_\nu^{(\omega_0)}}\mu_{z,\nu}^{(\omega_0)}\delta(x-x_\nu)\frac{\partial}{\partial y}\delta(y-y_\nu),$$

$$\bar{E}_{y,\nu+\epsilon}-\bar{E}_{y,\nu-\epsilon}=-\frac{1}{\epsilon_0\bar{\epsilon}_\nu^{(\omega_0)}}\mu_{z,\nu}^{(\omega_0)}\delta(y-y_\nu)\frac{\partial}{\partial x}\delta(x-x_\nu). \tag{62}$$

In the calculations leading to these equations, the identity

$$\nabla\times\delta(\boldsymbol{r}-\boldsymbol{r}_\nu)\hat{z}=\left[\frac{\partial}{\partial y}\delta(\boldsymbol{r}-\boldsymbol{r}_\nu),-\frac{\partial}{\partial x}\delta(\boldsymbol{r}-\boldsymbol{r}_\nu),0\right]$$

was used. Furthermore, the terms containing the discontinuities and singularities of the type of the Dirac δ function in the x and y dimensions were omitted since they do not contribute to the boundary conditions, as discussed in Sec. II D 3.

The first equation in Eq. (62) implies the continuity of the tangential components of the vector $\bar{\boldsymbol{E}}$ everywhere except at the location of the point dipole. This is equivalent to the well-known boundary condition for the medium containing no free charge currents. The influence of the point dipole is described by the second and third equations. In particular, the discontinuities of the x and y components of the field $\bar{\boldsymbol{E}}$ at the location of the point dipole are determined by the right-hand sides of the second and third equations, respectively.

When boundary conditions (62) are expressed in the $\boldsymbol{q}$ space, the following equations are found:

$$\Delta\bar{\mathcal{E}}_{x,\nu,\Sigma,\Sigma}\equiv\bar{\mathcal{E}}_{x,\nu+\epsilon,\Sigma,\Sigma}-\bar{\mathcal{E}}_{x,\nu-\epsilon,\Sigma,\Sigma}=-ik_x\frac{(k_0^u)^2}{\epsilon_0\bar{\epsilon}_\nu^{(\omega_0)}}\mu_{z,\nu}^{(\omega_0)}\exp[-i\boldsymbol{q}\cdot\boldsymbol{\rho}_\nu],$$

$$\Delta\bar{\mathcal{E}}_{y,\nu,\Sigma,\Sigma}\equiv\bar{\mathcal{E}}_{y,\nu+\epsilon,\Sigma,\Sigma}-\bar{\mathcal{E}}_{y,\nu-\epsilon,\Sigma,\Sigma}=-ik_y\frac{(k_0^u)^2}{\epsilon_0\bar{\epsilon}_\nu^{(\omega_0)}}\mu_{z,\nu}^{(\omega_0)}\exp[-i\boldsymbol{q}\cdot\boldsymbol{\rho}_\nu]. \tag{63}$$

These equations provide explicit expressions for the magnitudes of the discontinuities of the x and y components of the vector $\bar{\boldsymbol{\mathcal{E}}}_{\nu,\Sigma,\Sigma}$ at the location of the oscillating dipole.

3. Matrix representation of the boundary conditions in the q space

As mentioned earlier, equations $\bar{\boldsymbol{D}}=\epsilon_0\bar{\epsilon}_\nu^{(\omega_0)}\bar{\boldsymbol{E}}$ and $\bar{\boldsymbol{B}}=\mu_0\bar{\boldsymbol{H}}$ are valid everywhere in the medium characterized by the macroscopic permittivity $\bar{\epsilon}_\nu^{(\omega_0)}$. Using the latter equation and the Maxwell equation (3b), one can derive a relation between the vector modal amplitudes $\bar{\boldsymbol{\mathcal{E}}}_{\nu,\Sigma,d}$ and $\bar{\boldsymbol{\mathcal{H}}}_{\nu,\Sigma,d}$ in the form $\bar{N}_{\nu,p,d}\times\bar{\boldsymbol{\mathcal{E}}}_{\nu,\Sigma,d}=\eta_0\bar{\boldsymbol{\mathcal{H}}}_{\nu,\Sigma,d}$. In an isotropic medium, which is considered here, the wave vectors $\bar{N}_{\nu,p,d}$ are equivalent for both polarization states $p=1,2$, as follows from Eq. (30). Consequently, the boundary conditions for the field vectors $\bar{\boldsymbol{\mathcal{E}}}$ and $\bar{\boldsymbol{\mathcal{H}}}$ expressed in the $\boldsymbol{q}$ space can be written in a compact matrix form[37]

$$\begin{bmatrix}\Delta\bar{\mathcal{E}}_{x,\nu,\Sigma,\Sigma}\\ \eta_0\Delta\bar{\mathcal{H}}_{y,\nu,\Sigma,\Sigma}\\ \eta_0\Delta\bar{\mathcal{H}}_{z,\nu,\Sigma,\Sigma}\\ \eta_0\Delta\bar{\mathcal{H}}_{x,\nu,\Sigma,\Sigma}\\ \Delta\bar{\mathcal{E}}_{y,\nu,\Sigma,\Sigma}\\ \Delta\bar{\mathcal{E}}_{z,\nu,\Sigma,\Sigma}\end{bmatrix}=\begin{bmatrix}1&1&0&0&0&0\\ \bar{N}_{z,\nu,+}^{(\omega_0)}&\bar{N}_{z,\nu,-}^{(\omega_0)}&0&0&-N_x^{(\omega_0)}&-N_x^{(\omega_0)}\\ -N_y^{(\omega_0)}&-N_y^{(\omega_0)}&N_x^{(\omega_0)}&N_x^{(\omega_0)}&0&0\\ 0&0&-\bar{N}_{z,\nu,+}^{(\omega_0)}&-\bar{N}_{z,\nu,-}^{(\omega_0)}&N_y^{(\omega_0)}&N_y^{(\omega_0)}\\ 0&0&1&1&0&0\\ 0&0&0&0&1&1\end{bmatrix}\begin{bmatrix}\Delta\bar{\mathcal{E}}_{x,\nu,\Sigma,+}\\ \Delta\bar{\mathcal{E}}_{x,\nu,\Sigma,-}\\ \Delta\bar{\mathcal{E}}_{y,\nu,\Sigma,+}\\ \Delta\bar{\mathcal{E}}_{y,\nu,\Sigma,-}\\ \Delta\bar{\mathcal{E}}_{z,\nu,\Sigma,+}\\ \Delta\bar{\mathcal{E}}_{z,\nu,\Sigma,-}\end{bmatrix}$$

$$=\frac{-ik_0^{(\omega_0)}(k_0^u)^2}{\bar{\epsilon}_\nu^{(\omega_0)}\epsilon_0}\exp[-i\boldsymbol{q}\cdot\boldsymbol{\rho}_\nu]\begin{bmatrix}N_x^{(\omega_0)}\mu_{z,\nu}^{(\omega_0)}\\ -\mu_{x,\nu}^{(\omega_0)}\bar{\epsilon}_\nu^{(\omega_0)}\\ 0\\ \mu_{y,\nu}^{(\omega_0)}\bar{\epsilon}_\nu^{(\omega_0)}\\ N_y^{(\omega_0)}\mu_{z,\nu}^{(\omega_0)}\\ N_x^{(\omega_0)}\mu_{x,\nu}^{(\omega_0)}+N_y^{(\omega_0)}\mu_{y,\nu}^{(\omega_0)}\end{bmatrix}, \tag{64}$$

where $\Delta\bar{\mathcal{E}}_{x,\nu,\Sigma,\pm}\equiv\bar{\mathcal{E}}_{x,\nu+\epsilon,\Sigma,\pm}-\bar{\mathcal{E}}_{x,\nu-\epsilon,\Sigma,\pm}$, and similarly for the y and z components. Equation (64) provides an important result: it shows explicitly the relation between the discontinuities of the vector modal amplitudes at the location of the point dipole, i.e., at $\boldsymbol{r}=\boldsymbol{r}_\nu$, and the strength of the point dipole $\boldsymbol{\mu}_\nu^{(\omega_0)}$ for a mode characterized by the vector $\boldsymbol{q}=k_0^{(\omega_0)}[N_x,N_y]$.

The 6×6 matrix in Eq. (64) is singular and thus the equation cannot be solved in the form as it stands now. This agrees with the fact that the x, y, and z components of the vectors $\bar{\boldsymbol{\mathcal{E}}}_{\nu,\Sigma,\pm}$, and thus the vectors $\Delta\bar{\boldsymbol{\mathcal{E}}}_{\nu,\Sigma,\pm}$, are not independent of each other.

In particular, if we consider the **s**- and **p**-polarized modes with the corresponding magnitudes $\overline{\mathcal{E}}^{(\omega_0)}_{\nu,\mathbf{s},\pm}$ and $\overline{\mathcal{E}}^{(\omega_0)}_{\nu,\mathbf{p},\pm}$ and assume that the x component of the normalized wave vector $\overline{\boldsymbol{N}}^{(\omega_0)}_{\nu,\pm}$ is equal to zero, then the y and z components of the vector modal amplitudes $\overline{\boldsymbol{\mathcal{E}}}_{\nu,\mathbf{p},\pm}$ are not independent but related as $\overline{\mathcal{E}}^{(\omega_0)}_{y,\nu,\mathbf{p},\pm}/\overline{\mathcal{E}}^{(\omega_0)}_{z,\nu,\mathbf{p},\pm}=-(\overline{N}^{(\omega_0)}_{z,\nu,\pm}/\overline{N}^{(\omega_0)}_{y,\nu})$, as follows from Eqs. (30)–(32) where ω is substituted by $\omega_0=2\omega$. Considering this relation and removing all linearly dependent columns and rows of the 6×6 matrix in Eq. (64), the boundary conditions can be written as

$$\begin{bmatrix} \Delta\overline{\mathcal{E}}_{x,\nu,\Sigma,\Sigma} \\ \eta_0\Delta\overline{\mathcal{H}}_{y,\nu,\Sigma,\Sigma} \\ \Delta\overline{\mathcal{E}}_{y,\nu,\Sigma,\Sigma} \\ \eta_0\Delta\overline{\mathcal{H}}_{x,\nu,\Sigma,\Sigma} \end{bmatrix} = \begin{bmatrix} 1 & 1 & 0 & 0 \\ \overline{N}^{(\omega_0)}_{z,\nu,+} & \overline{N}^{(\omega_0)}_{z,\nu,-} & 0 & 0 \\ 0 & 0 & \overline{N}^{(\omega_0)}_{z,\nu,+}/\overline{N}^{(\omega_0)}_{\nu} & \overline{N}^{(\omega_0)}_{z,\nu,-}/\overline{N}^{(\omega_0)}_{\nu} \\ 0 & 0 & -\overline{N}^{(\omega_0)}_{\nu} & -\overline{N}^{(\omega_0)}_{\nu} \end{bmatrix} \begin{bmatrix} \Delta\overline{\mathcal{E}}_{\nu,\mathbf{s},+} \\ \Delta\overline{\mathcal{E}}_{\nu,\mathbf{s},-} \\ \Delta\overline{\mathcal{E}}_{\nu,\mathbf{p},+} \\ \Delta\overline{\mathcal{E}}_{\nu,\mathbf{p},-} \end{bmatrix}$$

$$= \frac{-ik_0^{(\omega_0)}(k_0^u)^2}{\overline{\epsilon}^{(\omega_0)}_{\nu}\epsilon_0}\exp[-i\boldsymbol{q}\cdot\boldsymbol{\rho}_\nu] \begin{bmatrix} 0 \\ -\overline{\epsilon}^{(\omega_0)}_{\nu}\mu^{(\omega_0)}_{x,\nu} \\ \overline{\epsilon}^{(\omega_0)}_{\nu}\mu^{(\omega_0)}_{y,\nu} \\ N^{(\omega_0)}_{y}\mu^{(\omega_0)}_{z,\nu} \end{bmatrix}. \tag{65}$$

This equation can already be solved since the 4×4 matrix is regular. This matrix is the dynamic matrix $\overline{D}^{(\omega_0)}_{\nu}$ defined in Eq. (33) which binds the modal magnitudes with the tangential components of the electrical and magnetic field. Taking into account that $\overline{N}^{(\omega_0)}_{z,\nu,+}=-\overline{N}^{(\omega_0)}_{z,\nu,-}=\overline{N}^{(\omega_0)}_{z,\nu}$, as shown in Eq. (30), the result is

$$\Delta\overline{\boldsymbol{A}}^{(\omega_0)}_{\nu}\equiv\begin{bmatrix} \Delta\overline{\mathcal{E}}_{\nu,\mathbf{s},+} \\ \Delta\overline{\mathcal{E}}_{\nu,\mathbf{s},-} \\ \Delta\overline{\mathcal{E}}_{\nu,\mathbf{p},+} \\ \Delta\overline{\mathcal{E}}_{\nu,\mathbf{p},-} \end{bmatrix} = \frac{-ik_0^{(\omega_0)}(k_0^u)^2}{2\overline{\epsilon}^{(\omega_0)}_{\nu}\epsilon_0}\exp[-i\boldsymbol{q}\cdot\boldsymbol{\rho}_\nu] \begin{bmatrix} -\dfrac{\overline{\epsilon}^{(\omega_0)}_{\nu}}{\overline{N}^{(\omega_0)}_{z,\nu}}\mu^{(\omega_0)}_{x,\nu} \\ \dfrac{\overline{\epsilon}^{(\omega_0)}_{\nu}}{\overline{N}^{(\omega_0)}_{z,\nu}}\mu^{(\omega_0)}_{x,\nu} \\ -\overline{N}^{(\omega_0)}_{\nu}\mu^{(\omega_0)}_{y,\nu}+\overline{N}^{(\omega_0)}_{\nu}\dfrac{N^{(\omega_0)}_{y}}{\overline{N}^{(\omega_0)}_{z,\nu}}\mu^{(\omega_0)}_{z,\nu} \\ -\overline{N}^{(\omega_0)}_{\nu}\mu^{(\omega_0)}_{y,\nu}-\overline{N}^{(\omega_0)}_{\nu}\dfrac{N^{(\omega_0)}_{y}}{\overline{N}^{(\omega_0)}_{z,\nu}}\mu^{(\omega_0)}_{z,\nu} \end{bmatrix}. \tag{66}$$

Considering again Eqs. (30)–(32), the components of the vector $\Delta\overline{\boldsymbol{A}}^{(\omega_0)}_{\nu}$ defined in Eq. (66) can be rewritten in a more compact and general forms as

$$\Delta\overline{\mathcal{E}}_{\nu,\mathbf{s},\pm}=\frac{i(k_0^u)^2}{2\epsilon_0}\frac{k_0^{(\omega_0)}}{\pm\overline{N}^{(\omega_0)}_{z,\nu}}(\boldsymbol{\mu}^{(\omega_0)}_{\nu}\cdot\hat{\boldsymbol{e}}^{(\omega_0)}_{\nu,\mathbf{s},\pm})\exp[-i\boldsymbol{q}\cdot\boldsymbol{\rho}_\nu],$$

$$\Delta\overline{\mathcal{E}}_{\nu,\mathbf{p},\pm}=\frac{i(k_0^u)^2}{2\epsilon_0}\frac{k_0^{(\omega_0)}}{\pm\overline{N}^{(\omega_0)}_{z,\nu}}(\boldsymbol{\mu}^{(\omega_0)}_{\nu}\cdot\hat{\boldsymbol{e}}^{(\omega_0)}_{\nu,\mathbf{p},\pm})\exp[-i\boldsymbol{q}\cdot\boldsymbol{\rho}_\nu]. \tag{67}$$

This is the final result of this section. It provides explicit formulas for the discontinuities of the magnitudes of the **s**- and **p**-polarized modes expressed in the $\boldsymbol{q}$ space at the position of the point dipole (i.e. at the point $\boldsymbol{r}=\boldsymbol{r}_\nu$) inside the medium of permittivity $\overline{\epsilon}^{(\omega_0)}_{\nu}$. This result will be used later in the matrix formalism describing the propagation of the SH field across the multilayer system.

4. Propagation of the dipole-generated SH field across the multilayer structure

In the previous section, we derived the boundary conditions in the presence of an oscillating point electric dipole located at the position $\boldsymbol{r}=\boldsymbol{r}_\nu$. In this section we incorporate the obtained formulas into the matrix formalism describing the propagating of the SH field across the multilayer structure.

As mentioned at the beginning of Sec. II F, it is assumed that the oscillating point dipole is located inside an infinitesimally thin vacuum layer (i.e., $\overline{\epsilon}^{(\omega_0)}_{\nu}=\epsilon_{\mathrm{vac}}=1$) which is inserted at the location of the νth interface, as shown in Fig. 3. Within this layer, the EM field can be decomposed into **s** and **p** modes. The magnitudes of these modes at the position immediately below and above the dipole location (but still

inside the thin vacuum sheet) are contained in the vectors denoted by $\overline{\boldsymbol{A}}^{(2\omega)}_{\nu+\epsilon}$ and $\overline{\boldsymbol{A}}^{(2\omega)}_{\nu-\epsilon}$, respectively, as shown in Fig. 3. Using this notation, the discontinuity of the field at the location of the point dipole can be written as

$$\overline{\boldsymbol{A}}^{(2\omega)}_{\nu+\epsilon}-\overline{\boldsymbol{A}}^{(2\omega)}_{\nu-\epsilon}=\Delta\overline{\boldsymbol{A}}^{(2\omega)}_{\nu}, \tag{68}$$

where $\Delta\overline{\boldsymbol{A}}^{(2\omega)}_{\nu}$ is given by Eqs. (66) and (67). The overbar refers to the fact that these variables are inside the thin vacuum sheet. This also has to be reflected in Eqs. (66) and (67) where all the quantities depending on the permittivity $\overline{\epsilon}^{(\omega_0)}_{\nu}$, namely, $\overline{N}^{(\omega_0)}_{z,\nu}$, $\hat{\overline{\boldsymbol{e}}}^{(\omega_0)}_{\nu,\mathbf{s},\pm}$, and $\hat{\overline{\boldsymbol{e}}}^{(\omega_0)}_{\nu,\mathbf{p},\pm}$, should be substituted by their corresponding vacuum equivalents.

Applying the matrix formalism developed in Sec. II E, the vectors $\overline{\boldsymbol{A}}^{(2\omega)}_{\nu\pm\epsilon}$ are related to the vectors $\boldsymbol{A}^{(2\omega)}_{0}$ and $\boldsymbol{A}^{(2\omega)}_{M+1}$ by [refer to Eqs. (37) and (39) and Fig. 3]

$$\boldsymbol{A}^{(2\omega)}_{0}=L^{(2\omega)}_{\nu}[D^{(2\omega)}_{\nu}]^{-1}D^{(2\omega)}_{\mathrm{vac}}\overline{\boldsymbol{A}}^{(2\omega)}_{\nu-\epsilon} \tag{69}$$

and

$$\overline{\boldsymbol{A}}^{(2\omega)}_{\nu+\epsilon}=[D^{(2\omega)}_{\mathrm{vac}}]^{-1}D^{(2\omega)}_{\nu}[L^{(2\omega)}_{\nu}]^{-1}L^{(2\omega)}_{M+1}\boldsymbol{A}^{(2\omega)}_{M+1}, \tag{70}$$

where the matrices $L^{(2\omega)}_{\nu}$, $D^{(2\omega)}_{\nu}$ and $D^{(2\omega)}_{\mathrm{vac}}$ are calculated in a similar way as their fundamental counterparts in Sec. II E upon the substitution $\omega\rightarrow 2\omega$.

Combining Eqs. (68)–(70), we can write

$$\boldsymbol{A}^{(2\omega)}_{0}=L^{(2\omega)}_{M+1}\boldsymbol{A}^{(2\omega)}_{M+1}-L^{(2\omega)}_{\nu}[D^{(2\omega)}_{\nu}]^{-1}D^{(2\omega)}_{\mathrm{vac}}\Delta\overline{\boldsymbol{A}}^{(2\omega)}_{\nu}. \tag{71}$$

This equation is a crucial result of our analysis since it provides an explicit relation between the magnitudes of the modes of the SH field propagating in the superstrate (contained in the vector $\boldsymbol{A}^{(2\omega)}_{0}$) and substrate (contained in the vector $\boldsymbol{A}^{(2\omega)}_{M+1}$) in the presence of an oscillating point electric dipole located at $\boldsymbol{r}=\boldsymbol{r}_{\nu}$. This equation is also a generalization of formula (39), which is valid only in a charge-free multilayer system.

Because the SH field is generated only within the multilayer structure, the vectors $\boldsymbol{A}^{(2\omega)}_{0}$ and $\boldsymbol{A}^{(2\omega)}_{M+1}$ must take the forms

$$\boldsymbol{A}^{(2\omega)}_{0}=[0,\mathcal{E}^{(2\omega)}_{0,\mathbf{s},-},0,\mathcal{E}^{(2\omega)}_{0,\mathbf{p},-}],$$

$$\boldsymbol{A}^{(2\omega)}_{M+1}=[\mathcal{E}^{(2\omega)}_{M+1,\mathbf{s},+},0,\mathcal{E}^{(2\omega)}_{M+1,\mathbf{p},+},0]. \tag{72}$$

Thus the relationship between the modal magnitudes of the radiated SH field and the discontinuity $\Delta\overline{\boldsymbol{A}}^{(2\omega)}_{\nu}$ [see Eq. (66)] can be written as

$$\boldsymbol{A}^{(2\omega)}_{\nu,\mathrm{spd}}\equiv[\mathcal{E}^{(2\omega)}_{M+1,s+},\mathcal{E}^{(2\omega)}_{0,s-},\mathcal{E}^{(2\omega)}_{M+1,p+}\mathcal{E}^{(2\omega)}_{0,p-}]^{\mathrm{T}}=\mathbb{X}^{(2\omega)}_{\nu}\Delta\overline{\boldsymbol{A}}^{(2\omega)}_{\nu}, \tag{73}$$

where the matrix $\mathbb{X}^{(2\omega)}_{\nu}$ is defined as the product

$$\mathbb{X}^{(2\omega)}_{\nu}\equiv[K^{(2\omega)}_{M+1}]^{-1}L^{(2\omega)}_{\nu}[D^{(2\omega)}_{\nu}]^{-1}D^{(2\omega)}_{\mathrm{vac}} \tag{74}$$

and the matrix $K^{(2\omega)}_{M+1}$ is defined as

$$K^{(2\omega)}_{M+1}=\begin{bmatrix} L^{(2\omega)}_{11,M+1} & 0 & L^{(2\omega)}_{13,M+1} & 0\\ L^{(2\omega)}_{21,M+1} & -1 & L^{(2\omega)}_{23,M+1} & 0\\ L^{(2\omega)}_{31,M+1} & 0 & L^{(2\omega)}_{33,M+1} & 0\\ L^{(2\omega)}_{41,M+1} & 0 & L^{(2\omega)}_{43,M+1} & -1 \end{bmatrix}. \tag{75}$$

The subscript ''spd'' of the vector $\boldsymbol{A}^{(2\omega)}_{\nu,\mathrm{spd}}$, which is defined in Eq. (73), refers to the fact that the vector represents the radiated SH field generated by the *single point dipole*. Using Eq. (73), one can obtain the modal magnitudes of the SH field propagating in the superstrate and substrate by taking the elements of the vector $\boldsymbol{A}^{(2\omega)}_{\nu,\mathrm{spd}}$ with subscripts 0 and $M+1$, respectively.

Equation (73) is parametrized by $N^{(2\omega)}_{y}$, as follows from the quantities contained therein. More specifically, it provides the expression for the magnitudes of the **s**- and **p**-polarized SH modes propagating in the surrounding media in a particular direction characterized by $N^{(2\omega)}_{y}$, i.e., at particular angles $\theta^{(2\omega)}_{0}$ and $\theta^{(2\omega)}_{M+1}$ [see Fig. 2(b)]. These angles can be calculated from

$$N^{(2\omega)}_{y}=\sqrt{\epsilon^{(2\omega)}_{0}}\sin\theta^{(2\omega)}_{0}=\sqrt{\epsilon^{(2\omega)}_{M+1}}\sin\theta^{(2\omega)}_{M+1}. \tag{76}$$

G. Total second-harmonic far field

In the previous section, we derived the expressions for the SH radiation produced by a single point dipole located at a particular point at the νth interface of the multilayer system. Now, we exploit these results and derive the expressions for the SH field generated by the dipoles distributed over *all interfaces* of the multilayer system.

Before the derivation proceeds, we look closer at expression (2) for the point dipole generated by the fundamental field. Equation (46) suggests that the total fundamental field at the position of the dipole (i.e., at the νth interface) is a function of the lateral coordinate y. This function has a factorized form $\boldsymbol{E}^{(\omega)}_{\nu,\mathrm{int}}(y)=\tilde{\boldsymbol{E}}^{(\omega)}_{\nu,\mathrm{int}}(N^{(\omega)}_{y})\exp[ik^{(\omega)}_{0}N^{(\omega)}_{y}y]$, where the vector amplitude $\tilde{\boldsymbol{E}}^{(\omega)}_{\nu,\mathrm{int}}$ is parametrized by the direction of the incident fundamental beam, which is characterized by $N^{(\omega)}_{y}$. The exponential function describes the variation of the *phase* of the fundamental field with the lateral coordinate y, which is due to the propagation of the fundamental field along the multilayer structure.

As follows from expression (2), another quantity determining the amplitude of the point dipole is the nonlinear susceptibility tensor χ_{ν}. In general, each element of this tensor can have, due to various reasons which will be discussed in detail at the end of this section, a unique dependence on the lateral coordinate.

Although, in general, the dependence on both x and y should be considered, we restrict ourselves to the case where the susceptibility tensor depends only on y, i.e., $\chi_{\nu}(y)$. This is mainly due to the fact that only the light beams propagating in the y-z plane are treated in this paper. To facilitate the general case, i.e., to include the dependence of χ_{ν} on both x and y, the three-dimensional description of the SH field would have to be employed. This would involve introducing a nonzero x component of the normalized wave vector for the SH field, $N^{(2\omega)}_{x}\neq 0$. It would lead to more elaborate expressions for the solution of the wave equation (23), i.e., $\hat{\boldsymbol{e}}^{(2\omega)}_{\nu,p,d}(N^{(2\omega)}_{x},N^{(2\omega)}_{y})$, $N^{(2\omega)}_{z,\nu,p,d}(N^{(2\omega)}_{x},N^{(2\omega)}_{y})$, and thus to

more complicated expressions for the dynamic matrix $D_\nu^{(2\omega)}$ and the matrix $L_\nu^{(2\omega)}$. On the other hand, formula (67) representing the boundary conditions in the presence of a radiating point dipole is correct even for $N_x^{(2\omega)} \neq 0$, although it was determined for $N_x^{(2\omega)} = 0$.

Considering that the susceptibility tensors χ_ν do not depend on x, the variation of the point dipole $\boldsymbol{\mu}_\nu^{(2\omega)}$ in Eq. (2), with respect to y, can be written as

$$\boldsymbol{\mu}_\nu^{(2\omega)} = \tilde{\boldsymbol{\mu}}_\nu^{(2\omega)}(\chi_\nu(y), N_y^{(\omega)}) \exp[2ik_0^{(\omega)} N_y^{(\omega)} y], \tag{77}$$

where

$$\tilde{\boldsymbol{\mu}}_\nu^{(2\omega)}(\chi_\nu(y), N_y^{(\omega)}) \equiv \chi_\nu(y) \otimes \tilde{\boldsymbol{E}}_{\nu,\mathrm{int}}^{(\omega)}(N_y^{(\omega)}) \tilde{\boldsymbol{E}}_{\nu,\mathrm{int}}^{(\omega)}(N_y^{(\omega)}). \tag{78}$$

The first term in Eq. (77) represents the variation of the dipole *complex amplitude*, which is due to the lateral variation of the susceptibility tensor. The second (exponential) term in Eq. (77) represents the variation of the dipole *phase*, which is due to the variation of the phase of the incident fundamental field.

In expression (67), the unity vectors $\hat{\boldsymbol{e}}_{\nu,\mathbf{s},\pm}^{(2\omega)}$ and $\hat{\boldsymbol{e}}_{\nu,\mathbf{p},\pm}^{(2\omega)}$ are parametrized by the direction of observation of the SH field, which is characterized by $N_y^{(2\omega)}$. This follows from Eq. (32), where ω is substituted by 2ω. When the dependence of $\tilde{\boldsymbol{\mu}}_\nu^{(2\omega)}$ on y and $N_y^{(\omega)}$ expressed by Eq. (78) is taken into account, the quantities $\Delta\overline{\mathcal{E}}_{\nu,\mathbf{s},\pm}$ and $\Delta\overline{\mathcal{E}}_{\nu,\mathbf{p},\pm}$ in Eq. (67) can be written as

$$\Delta\overline{\mathcal{E}}_{\nu,\mathbf{s},\pm} = \Delta\widetilde{\overline{\mathcal{E}}}_{\nu,\mathbf{s},\pm}(\chi_\nu(y), N_y^{(\omega)}, N_y^{(2\omega)}) \exp[2ik_0^{(\omega)} N_y^{(\omega)} y], \tag{79}$$

where

$$\Delta\widetilde{\overline{\mathcal{E}}}_{\nu,\mathbf{s},\pm}(\chi_\nu(y), N_y^{(\omega)}, N_y^{(2\omega)}) \equiv \frac{i(k_0^u)^2}{2\epsilon_0} \frac{k_0^{(2\omega)}}{\pm \overline{N}_{z,\nu}^{(2\omega)}} \tilde{\boldsymbol{\mu}}_\nu^{(2\omega)}(\chi_\nu(y), N_y^{(\omega)}) \cdot \hat{\boldsymbol{e}}_{\nu,\mathbf{s},\pm}^{(2\omega)}(N_y^{(2\omega)}), \tag{80}$$

and similarly for the magnitudes of the **p**-polarized field. Consequently, the vector $\Delta\overline{\boldsymbol{A}}_\nu^{(2\omega)}$ defined in Eq. (66) can be written as $\Delta\overline{\boldsymbol{A}}_\nu^{(2\omega)} = \Delta\widetilde{\overline{\boldsymbol{A}}}_\nu^{(2\omega)}(\chi_\nu(y), N_y^{(\omega)}, N_y^{(2\omega)}) \times \exp[2ik_0^{(\omega)} N_y^{(\omega)} y]$, where the vector $\Delta\widetilde{\overline{\boldsymbol{A}}}_\nu^{(2\omega)}(\chi_\nu(y), N_y^{(\omega)}, N_y^{(2\omega)})$ is obtained from Eq. (66) in such a way that each element is substituted by its corresponding quantity given by Eq. (80).

The above analysis directly implies that every element of the vector on the left-hand side of Eq. (73) depends on the lateral coordinate y as well as on the quantities $N_y^{(\omega)}$ and $N_y^{(2\omega)}$. Therefore, the vector $\boldsymbol{A}_{\nu,\mathrm{spd}}^{(2\omega)}$ in Eq. (73) can be written as

$$\boldsymbol{A}_{\nu,\mathrm{spd}}^{(2\omega)} = \tilde{\boldsymbol{A}}_{\nu,\mathrm{spd}}^{(2\omega)}(\chi_\nu(y), N_y^{(\omega)}, N_y^{(2\omega)}) \exp[2ik_0^{(\omega)} N_y^{(\omega)} y], \tag{81}$$

where

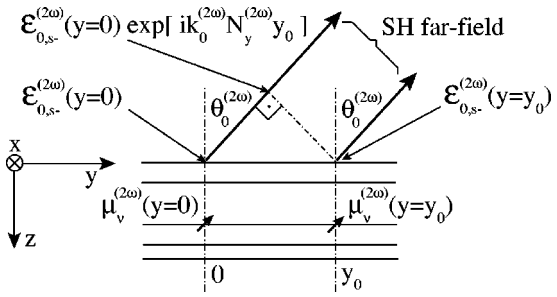

FIG. 4. Geometrical demonstration of the argument that the contributions to the SH far-field intensity originating from point dipoles at $y=0$ and $y=y_0$ are phase shifted by $\Delta\phi^{(2\omega)} = k_0^{(2\omega)} N_y^{(2\omega)} y_0$, where $N_y^{(2\omega)}$ characterizes the direction of propagation of the SH field [see Eq. (76)].

$$\tilde{\boldsymbol{A}}_{\nu,\mathrm{spd}}^{(2\omega)}(\chi_\nu(y), N_y^{(\omega)}, N_y^{(2\omega)}) \equiv \mathbb{X}_\nu^{(2\omega)}(N_y^{(2\omega)}) \cdot \Delta\tilde{\boldsymbol{A}}_{\mathrm{vac}}^{(2\omega)}(\chi_\nu(y), N_y^{(\omega)}, N_y^{(2\omega)}), \tag{82}$$

and the matrix $\mathbb{X}_\nu^{(2\omega)}(N_y^{(2\omega)})$ is defined in Eq. (74). Equation (82) is a compact form of Eq. (73), where the dependences on y, $N_y^{(\omega)}$ and $N_y^{(2\omega)}$ of the quantities contained therein are written explicitly.

To obtain the formula for the complex amplitude of the SH field radiated by the point dipoles distributed along the νth interface, one has to integrate the single dipole contributions (8) over the region where the dipoles are generated. In practical situations, the SH field is detected in the far-field configuration. This means that one usually measures the intensity of a plane SH wave propagating in the direction characterized by $N_y^{(2\omega)}$ [see Eq. (76)]. Due to the dependence of the phase of the fundamental field on y [see Eq. (46)], the integration over the νth interface has to be performed with care.

As can be seen from Fig. 4, the contribution to the far-field electric field originating from a dipole at $y=0$ exhibits a phase shift of $\Delta\phi^{(2\omega)} = k_0^{(2\omega)} N_y^{(2\omega)} y_0$ with respect to the contribution originating from a dipole at $y=y_0$. In order to take this into account, one has to consider the phase shift $\Delta\phi^{(2\omega)}$ when integrating the point dipole contributions along the νth interface.

In this analysis, the dipoles are assumed to be oscillating coherently, i.e., there is no disruption of the phase of the dipole oscillations along y. Furthermore, the magnitude of the fundamental field is assumed to be constant along the νth interface, which corresponds to the illumination of the multilayer system by an unbound plane wave. Consequently, the above geometrical argument implies that the SH far field originating from the dipoles located at the νth interface can be calculated as

$$\boldsymbol{A}_{\nu,\mathrm{iface}}^{(2\omega)}(N_y^{(\omega)}, N_y^{(2\omega)}) = \int_{-\infty}^{\infty} \mathrm{d}y \tilde{\boldsymbol{A}}_{\nu,\mathrm{spd}}^{(2\omega)}(\chi_\nu(y), N_y^{(\omega)}, N_y^{(2\omega)}) \times \exp[2ik_0^{(\omega)} N_y^{(\omega)} y - ik_0^{(2\omega)} N_y^{(2\omega)} y]. \tag{83}$$

The elements of the vector $\boldsymbol{A}^{(2\omega)}_{\nu,\mathrm{iface}}(N_y^{(\omega)},N_y^{(2\omega)})$, which is defined as[38]

$$\boldsymbol{A}^{(2\omega)}_{\nu,\mathrm{iface}} \equiv [\mathcal{E}^{(2\omega)}_{M+1,\mathbf{s},+,\mathrm{iface}},\mathcal{E}^{(2\omega)}_{0,\mathbf{s},-,\mathrm{iface}},\mathcal{E}^{(2\omega)}_{M+1,\mathbf{p},+,\mathrm{iface}},\mathcal{E}^{(2\omega)}_{0,\mathbf{p},-,\mathrm{iface}}]^{\mathrm{T}}, \tag{84}$$

represent the magnitudes of the **s**- and **p**-polarized modes propagating in the superstrate (subscript 0) and the substrate (subscript $M+1$) at the direction characterized by $N_y^{(2\omega)}$, and originating from the entire νth *interface* (hence the subscript ''iface''). Equation (83) provides the core result of the analysis presented in this paper.

The total radiated SH field, i.e., the SH field consisting of contributions from all interfaces of the multilayer system, is calculated simply by summing all the interface contributions (83), i.e.,

$$\boldsymbol{A}^{(2\omega)}_{\mathrm{mls}}(N_y^{(\omega)},N_y^{(2\omega)}) = \sum_{\nu=1}^{M+1} \boldsymbol{A}^{(2\omega)}_{\nu,\mathrm{iface}}(N_y^{(\omega)},N_y^{(2\omega)}). \tag{85}$$

Again, coherent radiation of the dipoles located at various interfaces was assumed in this step. In a similar way as for the vector $\boldsymbol{A}^{(2\omega)}_{\nu,\mathrm{iface}}$ in Eq. (84), the elements of the vector $\boldsymbol{A}^{(2\omega)}_{\mathrm{mls}}(N_y^{(\omega)},N_y^{(2\omega)})$, which is defined as[38]

$$\boldsymbol{A}^{(2\omega)}_{\mathrm{mls}} \equiv [\mathcal{E}^{(2\omega)}_{M+1,\mathbf{s},+,\mathrm{mls}},\mathcal{E}^{(2\omega)}_{0,\mathbf{s},-,\mathrm{mls}},\mathcal{E}^{(2\omega)}_{M+1,\mathbf{p},+,\mathrm{mls}},\mathcal{E}^{(2\omega)}_{0,\mathbf{p},-,\mathrm{mls}}]^{\mathrm{T}}, \tag{86}$$

represent the magnitudes of the **s** and **p** polarized modes propagating in the superstrate (subscript 0) and the substrate (subscript $M+1$) at the direction characterized by $N_y^{(2\omega)}$, and originating from the entire multilayer system (hence the subscript ''mls'').

H. Angular dependence of the second-harmonic far field

In Sec. II G, we derived the expressions for the total SH field generated within the multilayer system. It can be seen from Eqs. (83) and (85) that the expressions for the SH field are parametrized by $N_y^{(2\omega)}$. In other words, Eqs. (83) and (85) describe the angular dependence of the radiated SH field, as follows from Eq. (76). In this section, we analyze this angular distribution in greater detail.

Equation (83) is the fundamental expression describing the angular dependence of the SH far field generated by the νth interface. This equation suggests that the quantities $\boldsymbol{A}^{(2\omega)}_{\nu,\mathrm{iface}}(N_y^{(\omega)},N_y^{(2\omega)})$ and $\tilde{\boldsymbol{A}}^{(2\omega)}_{\nu,\mathrm{spd}}(\chi_\nu(y),N_y^{(\omega)},N_y^{(2\omega)})$ are related by Fourier transforms.

First, we note that $k_0^{(2\omega)} \equiv 2\omega/c_0 = 2k_0^{(\omega)}$. Second, we recall that the dependence of the vector $\tilde{\boldsymbol{A}}^{(2\omega)}_{\nu,\mathrm{spd}}(\chi_\nu(y),N_y^{(\omega)},N_y^{(2\omega)})$ on y is due to the lateral variation of the complex amplitude of the point dipole. This dependence is due to the variation of the nonlinear susceptibility tensor χ_ν along the interface, as follows from Eq. (78). Consequently, if we define the Fourier transform of the tensor $\chi_\nu(y)$ as[39]

$$\mathcal{FT}[\chi_\nu](u) \equiv \int_{-\infty}^{\infty} \mathrm{d}y\, \chi_\nu(y) \exp[iuy], \tag{87}$$

Eq. (83) can be rewritten as

$$\boldsymbol{A}^{(2\omega)}_{\nu,\mathrm{iface}}(N_y^{(\omega)},N_y^{(2\omega)}) = \mathcal{FT}[\tilde{\boldsymbol{A}}^{(2\omega)}_{\nu,\mathrm{spd}}](u,N_y^{(\omega)},N_y^{(2\omega)}), \tag{88}$$

where

$$u = 2k_0^{(\omega)}(N_y^{(\omega)} - N_y^{(2\omega)}). \tag{89}$$

Using Eq. (82), the vector $\mathcal{FT}[\tilde{\boldsymbol{A}}^{(2\omega)}_{\nu,\mathrm{spd}}](u,N_y^{(\omega)},N_y^{(2\omega)})$ in Eq. (88) is calculated as

$$\mathcal{FT}[\tilde{\boldsymbol{A}}^{(2\omega)}_{\nu,\mathrm{spd}}](u,N_y^{(\omega)},N_y^{(2\omega)}) = \mathbb{X}^{(2\omega)}_\nu(N_y^{(2\omega)}) \cdot \mathcal{FT}[\Delta\tilde{\boldsymbol{A}}^{(2\omega)}_\nu](u,N_y^{(\omega)},N_y^{(2\omega)}). \tag{90}$$

In this equation, the vector $\mathcal{FT}[\Delta\tilde{\boldsymbol{A}}^{(2\omega)}_\nu](u,N_y^{(\omega)},N_y^{(2\omega)})$ consists of the quantities

$$\mathcal{FT}[\Delta\tilde{\mathcal{E}}^{(2\omega)}_{\nu,p,\pm}](u,N_y^{(\omega)},N_y^{(2\omega)}) = \frac{i(k_0^u)^2}{2\epsilon_0} \frac{k_0^{(2\omega)}}{\pm\bar{N}^{(2\omega)}_{z,\nu}} \hat{\boldsymbol{e}}^{(2\omega)}_{\nu,p,d}(N_y^{(2\omega)}) \cdot \underline{\underline{\mathcal{FT}[\chi_\nu](u)}} \otimes \tilde{\boldsymbol{E}}^{(\omega)}_{\nu,\mathrm{int}}(N_y^{(\omega)}) \tilde{\boldsymbol{E}}^{(\omega)}_{\nu,\mathrm{int}}(N_y^{(\omega)}), \tag{91}$$

as follows from Eqs. (80) and (78) and definition (66).

Equations (85)–(91) provide quite a remarkable result—they establish the theoretical grounds for the analysis of the variation of the susceptibility tensor elements with the *lateral coordinate y* from the measurement of the *angular dependence* of the radiated SH far field. The importance of this becomes even more apparent when one realizes that the interface, which is the source of the SH field, can be any *buried* interface of the multilayer system.

Let us first assume that *none* of the elements of the nonlinear susceptibility tensors depend on y, i.e., $\chi_{ijk,\nu}(y) = \chi_{ijk,\nu}(0)$ for all y and for every ν. Equation (87) implies that the Fourier transform of the tensor elements is proportional to the Dirac δ function, i.e., $\mathcal{FT}[\chi_{ijk,\nu}](u) = \chi_{ijk,\nu}(0)\,\delta(u)$. Consequently, after substituting the result into Eqs. (88)–(91), the elements of the vector $\boldsymbol{A}^{(2\omega)}_{\nu,\mathrm{iface}}(N_y^{(\omega)},N_y^{(2\omega)})$ and consequently the magnitudes of the modes of the SH far field are found to be proportional to $\delta(N_y^{(\omega)} - N_y^{(2\omega)})$. A direct implication of this result is that the SH far field is nonzero only for such combinations of the incident and observation angles that the equation

$$N_y^{(\omega)} = N_y^{(2\omega)} \tag{92}$$

is satisfied. This agrees with a well-known experimental experience that the angle at which the SH far-field intensity is observed is the same as the incident angle of the fundamental beam.[5,8,9,31] This is, of course, true only when the SHG is performed in the reflection configuration within a nondispersive medium, i.e., when the fundamental beam enters the

multilayer structure from the same nondispersive medium as where the SH intensity is observed. If, for example, the fundamental field enters from the superstrate and the SH field is observed in the substrate, the angle of observation $\theta_{M+1}^{(2\omega)} = \arcsin(N_y^{(2\omega)}/\sqrt{\epsilon_{M+1}^{(2\omega)}})$ could be different from the incident angle $\theta_0^{(\omega)} = \arcsin(N_y^{(\omega)}/\sqrt{\epsilon_0^{(\omega)}})$ due to differences in the substrate and superstrate optical parameters, i.e., if $\epsilon_{M+1}^{(2\omega)} \neq \epsilon_0^{(\omega)}$. Furthermore, even if the SH field is observed in the same medium as that from which the fundamental field impinges the multilayer system, the observation angle could still be different from the incident one due to the material dispersion, i.e., if $\epsilon_0^{(2\omega)} \neq \epsilon_0^{(\omega)}$ or $\epsilon_{M+1}^{(2\omega)} \neq \epsilon_{M+1}^{(\omega)}$.

As follows from Eqs. (87) and (88), more interesting results can be obtained when some of the elements of the nonlinear susceptibility tensors $\chi_{ijk,\nu}$ vary with y. This could be due to various reasons. For example, in the area of magnetic-induced second-harmonic generation, the susceptibility tensor describing the nonlinear properties of some interface ν_0 depends on the local magnetization. Thus, if the magnetic medium neighboring this interface contains magnetic domains or any other lateral variations of the magnetization (such as propagating spin waves, magnetic nanostructures, etc., as discussed in Sec. II C) these variations will be directly reflected in the variations of the susceptibility tensor elements $\chi_{ijk,\nu_0}(y)$. This will, in turn, result in the dispersion of the tensor $\mathcal{FT}[\chi_{ijk,\nu_0}](u)$ in the Fourier domain, which will eventually result in the modification of the angular distribution of the SH far field, as described by Eqs. (85)–(91).

I. SH intensity in the far field

The analysis presented in the previous sections dealt exclusively with the expressions for the electromagnetic field vectors expressed in the $\boldsymbol{q}$ space. However, in order to obtain results which could directly be compared with experimental data, we need to calculate the SH far-field intensity in the $\boldsymbol{r}$ space. A typical SH experimental arrangement involves the measurement of the far-field intensity. Therefore, in this section we concentrate on the derivation of the far-field intensity radiated into the superstrate and substrate surrounding the multilayer system.

The fundamental relation between the $\boldsymbol{q}$ space, in which all the previous calculations were carried out, and the $\boldsymbol{r}$ space is provided by Eq. (6). As mentioned in the discussion after this equation, it is important to realize that the vector $\boldsymbol{\mathcal{E}}_{\boldsymbol{q},j,\Sigma,\Sigma}$ [recall notation (8)] depends on the z coordinate. In the case of the SH field propagating in the superstrate and substrate, this dependence can be explicitly written as

$$\boldsymbol{\mathcal{E}}_{\boldsymbol{q},j,\Sigma,\Sigma}^{(2\omega)} = \sum_{p,d} \mathcal{E}_{j,p,d,\mathrm{mls}}^{(2\omega)} \hat{\boldsymbol{e}}_{j,p,d}^{(2\omega)} \exp[ik_{z,j,d}^{(2\omega)}(z-z_j)], \quad (93)$$

where $j=0$ and $j=M+1$ correspond to the superstrate and the substrate, respectively. In this equation, it was considered that $k_{z,j,\mathbf{p},d}^{(2\omega)} = k_{z,j,\mathbf{s},d}^{(2\omega)} \equiv k_{z,j,d}^{(2\omega)}$ in an isotropic medium and the polarization vectors $\hat{\boldsymbol{e}}_{j,p,d}^{(2\omega)}$ are given by Eq. (32) upon substitution $\omega \to 2\omega$. Furthermore, the magnitudes $\mathcal{E}_{j,p,d,\mathrm{mls}}^{(2\omega)}$ are given in Eq. (86). It should be recalled that $\mathcal{E}_{j,p,d,\mathrm{mls}}^{(2\omega)}$ are nonzero only for the combination of indices $j=0$, $d=-$ and $j=M+1$, $d=+$.

Considering Eqs. (6) and (93), the total SH electric field generated within the multilayer system and radiated into the surrounding media can be written as

$$\boldsymbol{E}_{j,\Sigma,\Sigma,\mathrm{mls}}^{(2\omega)}(\boldsymbol{r}) = \frac{1}{(2\pi k_0^u)^2} \int\int \mathrm{d}^2\boldsymbol{q} \sum_{p,d} \boldsymbol{\mathcal{E}}_{j,p,d,\mathrm{mls}}^{(2\omega)} \times \exp[i\boldsymbol{\rho}\cdot\boldsymbol{q} + ik_{z,j,d}^{(2\omega)}(z-z_j)]. \quad (94)$$

To calculate this integral in the far-field, i.e., for $|\boldsymbol{r}| \gg \lambda^{(2\omega)}$, we employ the well-known method of stationary phase.[21,40] We carry out integration (94) in planar coordinates, in which one can write

$$\boldsymbol{r} \equiv \begin{bmatrix} x \\ y \\ z-z_j \end{bmatrix} = \begin{bmatrix} r\sin\theta_r\cos\varphi_r \\ r\sin\theta_r\sin\varphi_r \\ r\cos\theta_r \end{bmatrix},$$

$$\begin{bmatrix} k_x \\ k_y \\ k_z \end{bmatrix} = \begin{bmatrix} k^{(2\omega)}\sin\theta_k\cos\varphi_k \\ k^{(2\omega)}\sin\theta_k\sin\varphi_k \\ k^{(2\omega)}\cos\theta_k \end{bmatrix}, \quad (95)$$

where $[\theta_r, \varphi_r]$ and $[\theta_k, \varphi_k]$ are the angles characterizing the directions of the $\boldsymbol{r}$ and $\boldsymbol{k}^{(2\omega)} = [\boldsymbol{q}, k_z^{(2\omega)}]$ vectors, respectively. Considering Eq. (95), the phase in the exponential factor in Eq. (94) can be written as

$$\Phi(\boldsymbol{r}) = ik^{(2\omega)}r\{\cos(\theta_r-\theta_k) + [\cos(\varphi_r-\varphi_k)-1]\sin\theta_r\sin\theta_k\}, \quad (96)$$

and the differential $\mathrm{d}^2\boldsymbol{q}$ takes the form $\mathrm{d}^2\boldsymbol{q} = \mathrm{d}k_x\mathrm{d}k_y = (k^{(2\omega)})^2\cos\theta_k\sin\theta_k\mathrm{d}\theta_k\mathrm{d}\varphi_k$.

Employing the reasoning of the stationary phase method, the main contributions to integral (94) come from those points in the $\boldsymbol{q}$ space in which the phase $\Phi(\boldsymbol{r})$ is stationary, i.e., for which $\partial\Phi/\partial\theta_k = 0$ and $\partial\Phi/\partial\varphi_k = 0$ are fulfilled simultaneously. Using Eq. (96), these conditions are valid when $\theta_k = \theta_r$ and $\varphi_k = \varphi_r$, i.e., when the vectors $\boldsymbol{k}^{(2\omega)}$ and $\boldsymbol{r}$ are parallel. The Taylor expansion of the phase $\Phi(\boldsymbol{r})$ around this stationary point can consequently be written as

$$\Phi(\boldsymbol{r}) \approx ir k^{(2\omega)}\left[1 - \frac{1}{2}(\theta_k-\theta_r)^2 - \frac{\sin^2\theta_r}{2}(\varphi_k-\varphi_r)^2\right]. \quad (97)$$

When this approximation is substituted into Eq. (94), the integration can be carried out. After rather lengthy calculations which incorporate the same steps as in the stationary phase method,[21,40] we arrive at

$$\boldsymbol{E}_{j,\Sigma,d,\mathrm{mls}}^{(2\omega)}(\boldsymbol{r})\big|_{r\gg\lambda^{(2\omega)}} = \frac{2\pi k_j^{(2\omega)}}{(2\pi k_0^u)^2}\frac{1}{ir}\frac{N_{z,j}^{(2\omega)}}{N_j^{(2\omega)}}\boldsymbol{\mathcal{E}}_{j,\Sigma,d,\mathrm{mls}}^{(2\omega)}\exp[ik_j^{(2\omega)}r], \quad (98)$$

where we substituted $N_{z,j}^{(2\omega)}/N_j^{(2\omega)} = \cos\theta_{k,j}$.

To calculate the radiated SH intensity in the far-field, we simply use the definition $I(\boldsymbol{r})=|\langle \boldsymbol{S}(\boldsymbol{r})\rangle|$. Since the time-average of the Poynting vector $\boldsymbol{S}(\boldsymbol{r})$ is equal to[21,22] $\langle \boldsymbol{S}(\boldsymbol{r})\rangle = (1/2)\boldsymbol{E}(\boldsymbol{r})\times \boldsymbol{H}^{\star}(\boldsymbol{r})$, the SH intensity can be written as

$$I_j^{(2\omega)}(\boldsymbol{r}) \equiv I_j^{(2\omega)}(\boldsymbol{r};\theta_j^{(2\omega)},\varphi_j^{(2\omega)}) = \frac{1}{2\eta_0} N_j^{(2\omega)} |\boldsymbol{E}_{j,\Sigma,d,\mathrm{mls}}^{(2\omega)}(\boldsymbol{r})|^2$$

$$= \frac{1}{2\eta_0} \frac{(2\pi k_0^{(2\omega)})^2}{(2\pi k_0^u)^4} \frac{1}{r^2} N_j^{(2\omega)} |N_{z,j}^{(2\omega)}|^2$$

$$\times \sum_{p=\mathbf{s},\mathbf{p}} |\mathcal{E}_{j,p,d,\mathrm{mls}}^{(2\omega)}(\boldsymbol{q})|^2. \tag{99}$$

This is a final result of this section. It provides an explicit relation between the observable SH far-field intensity $I_j^{(2\omega)}(\boldsymbol{r})$ and the quantities $\mathcal{E}_{j,p,d,\mathrm{mls}}^{(2\omega)}(\boldsymbol{q})$ which are obtained from the matrix formalism developed in Secs. II E–II G. Equation (99) also provides an explicit relation between the measured intensity and the amplitude of the radiating point dipole. This explicit relationship can be used in the *quantitative* experimental determination of the amplitude of the point dipoles, $\boldsymbol{\mu}_\nu^{(2\omega)}$, which can be compared with *ab initio* calculations.

A number of comments should be made with regard to Eq. (99). First, it should be noted that since the amplitudes $\mathcal{E}_{j,p,d,\mathrm{mls}}^{(2\omega)}(\boldsymbol{q})$ are proportional to $(k_0^u)^2$, as follows from Eqs. (66)–(67) and (82)–(86), the overall intensity is *not* dependent on the arbitrary parameter k_0^u, as expected. Second, one should also observe that the intensity is proportional not only to the quantity $|\mathcal{E}_{j,p,d,\mathrm{mls}}^{(2\omega)}(\boldsymbol{q})|^2$ but rather to the product $|N_{z,j}^{(2\omega)}\mathcal{E}_{j,p,d,\mathrm{mls}}^{(2\omega)}(\boldsymbol{q})|^2$. The presence of the factor $|N_{z,j}^{(2\omega)}|^2$ originates from the fact that our formalism and consequently the magnitudes $\mathcal{E}_{j,p,d,\mathrm{mls}}^{(2\omega)}(\boldsymbol{q})$ are expressed in the $\boldsymbol{q}$ space. If we consider Eq. (15), which provides the relation between the $\boldsymbol{q}$ space and the $\boldsymbol{k}$ space, we find that in fact the far-field intensity is proportional to $|\mathcal{E}_{j,p,d,\mathrm{mls}}^{(2\omega)}(\boldsymbol{k})|^2$, i.e., to the modulus of the field magnitude expressed in the $\boldsymbol{k}$ space, which is an expected result.

Before concluding this section, it is also useful to provide some analytical results that could directly be compared with formulas available in the literature. For this purpose, let us consider that the multilayer system consists only of one planar interface separating the substrate and the superstrate whose refractive indices at the SH frequency are denoted by N_0 and N_1, respectively. Furthermore, let us assume that the fundamental field generates only a *single* point dipole of strength $\mu^{(2\omega)}$ and orientation in the y direction, i.e., $\boldsymbol{\mu}^{(2\omega)} = \mu^{(2\omega)}[0,1,0]$. When such a simple case is considered, the calculations presented in Secs. II E–II G lead to the expression

$$I_j^{(2\omega)}(\boldsymbol{r}) = \frac{c_0 (k_0^{(2\omega)})^4 (\mu^{(2\omega)})^2}{8\pi^2 \epsilon_0} \frac{(N_j)^3}{r^2} \left(\frac{N_{z,0} N_{z,1}}{N_0^2 N_{z,1} + N_1^2 N_{z,2}} \right)^2, \tag{100}$$

where $j=0,1$. This expression immediately implies that the ratio of the intensities radiated into the superstrate and substrate is equal to $(I_0^{(2\omega)}/I_1^{(2\omega)}) = (N_0/N_1)^3$, which is in agreement with the results published elsewhere.[24] Furthermore, if $N_0 = N_1 \equiv N$ is assumed, i.e., if the dipole is considered to be located in an homogeneous unbound medium of refractive index N, then expression (100)can be simplified to

$$I^{(2\omega)}(\boldsymbol{r}) = \frac{N c_0 (k_0^{(2\omega)})^4}{32\pi^2 \epsilon_0 r^2} (\mu^{(2\omega)} \cos\theta)^2, \tag{101}$$

which is the well-known cosinus law of radiation of a free point dipole treated in most textbooks on electromagnetism.[21,22]

Finally, it is worth noting that the expression for the far-field SH intensity was calculated for totally correlated point dipoles. In our derivations, the correlation of the radiating point dipoles is dictated by the correlation of the fundamental field, since the complex vector amplitude of the elementary dipoles is considered directly proportional to the fundamental field. We considered that the dipoles were generated by a plane wave, which is totally spatially correlated, and so the result in Eq. (99) corresponds to totally correlated point dipoles. Due to the point-dipole based approach, however, the formalism developed here could also be expanded towards uncorrelated or partially correlated dipoles. In principle, one would only need to add an appropriate correlation function describing the spatial correlation of the point dipoles into expressions (83) and (85) and then use the resulting formulas directly within the formalism of the theory of optical coherence.[29] The source of this partial correlation could be various. For example, it could be due to a partially correlated fundamental light generating the point dipoles. Another possibility is that some decorrelation mechanism is inherent in or enforced by an external influence upon the multilayer system or a specific layer or an interface. Even though steps in this direction would allow even further generalization and possibly wider applicability of our model, they will not be further pursued here as it would go beyond the scope of this paper.

III. NUMERICAL EXAMPLES

In this section, we apply the theory developed in Sec. II for the calculation of the SH far-field intensity generated by various multilayer systems. Because the results of this work are aimed at the analysis of magnetic-induced second harmonic generation (MSHG), in the following numerical examples we consider materials that are typically used in the MSHG experiments. Due to an enormous number of parameters involved in the MSHG phenomena, it is not feasible to consider all possible configurations or combinations of parameters. Therefore, we will focus on a few illustrative examples which demonstrate the features that one comes across during the studies of the MSHG in magnetic multilayer systems.

As mentioned in Sec. II, the nonlinear properties of the νth interface of a multilayer system are described by the susceptibility tensor $\chi_{ijk,\nu}$. Although there are, in general, 27 independent elements of the tensor $\chi_{ijk,\nu}$, the symmetry arguments applicable to the νth interface can reduce substan-

tially the number of its nonzero or independent elements. This procedure was thoroughly studied by other authors and can be found in the literature.[12,13]

In MSHG, the local magnetization $\mathcal{M}_\nu$ of the νth interface introduces breaking of the local symmetry, which has to be considered in addition to the restraints implied by the structural symmetry. In general, this results in an increased number of nonzero elements of the tensor $\chi_{ijk,\nu}$. Furthermore, the susceptibility tensor can be decomposed into two parts, one being odd and the other even in magnetization, i.e., $\chi_{ijk,\nu}=\chi^{(o)}_{ijk,\nu}+\chi^{(e)}_{ijk,\nu}$. In the first order of the magnetic perturbation, the even part contains the structural contribution and can be considered as independent on magnetization while the odd part can be considered as proportional to the magnetization. Thus by studying the values of the tensor $\chi^{(o)}_{ijk,\nu}$ via the second harmonic generation, one can probe for the local magnetization of the νth interface.

In Secs. II G–II H we derived that the SH intensity is a function of both the incident angle $\theta_i^{(\omega)}$ of the fundamental beam and the observation angle $\theta_o^{(2\omega)}$ of the SH field. Due to the above mentioned dependence of the susceptibility tensor on magnetization, the SH intensity also depends on magnetization $\mathcal{M}_\nu$, i.e., $I_o^{(2\omega)}(\theta_i^{(\omega)},\theta_o^{(2\omega)},\mathcal{M}_\nu)$. In this expression, $i=0$ or $i=M+1$, depending on whether the medium from which the fundamental field impinges on the multilayer system is the superstrate or substrate, respectively. Similarly, $o=0$ or $o=M+1$, depending on whether the medium where the SH field is observed is the superstrate or substrate, respectively.

In the area of MSHG, magnetic contrast is a convenient parameter for a quantification of the variation of the observed SH intensity with the magnetic field orientation. It is defined as

$$\rho_o(\theta_i^{(\omega)},\theta_o^{(2\omega)}) = \frac{I_o^{(2\omega)}(\theta_i^{(\omega)},\theta_o^{(2\omega)},\mathcal{M}_\nu)-I_o^{(2\omega)}(\theta_i^{(\omega)},\theta_o^{(2\omega)},-\mathcal{M}_\nu)}{I_o^{(2\omega)}(\theta_i^{(\omega)},\theta_o^{(2\omega)},\mathcal{M}_\nu)+I_o^{(2\omega)}(\theta_i^{(\omega)},\theta_o^{(2\omega)},-\mathcal{M}_\nu)}. \quad (102)$$

We will consider this parameter in our second numerical example.

Before we show the results, it is worth summarizing the steps that one needs to make in order to calculate the SH intensity. First, the material parameters (i.e., the permittivity tensors at the fundamental and SH frequencies and the susceptibility tensors) of the media comprising the multilayer structure must be known. Second, the distribution of the fundamental field across the multilayer system needs to be calculated. This can be done using Eqs. (43) or (44) derived in Sec. II E 3. Once the fundamental field is known, the distribution of point dipoles generating the SH field can be calculated from Eq. (2). The electric field generated by a point dipole propagating in the surrounding media can be calculated from Eq. (81) and (82), where the matrix $\mathbb{X}_\nu^{(2\omega)}$ and the vector $\Delta\tilde{\boldsymbol{A}}_\nu^{(2\omega)}$ are evaluated from Eqs. (74) and (66) and (67), respectively. When this result is integrated over a particular interface and summed over all interfaces, as shown in Eqs. (83) and (85), respectively, the total SH field is obtained. Finally, one should use Eq. (99) to obtain the angular variation of the observable SH intensity.

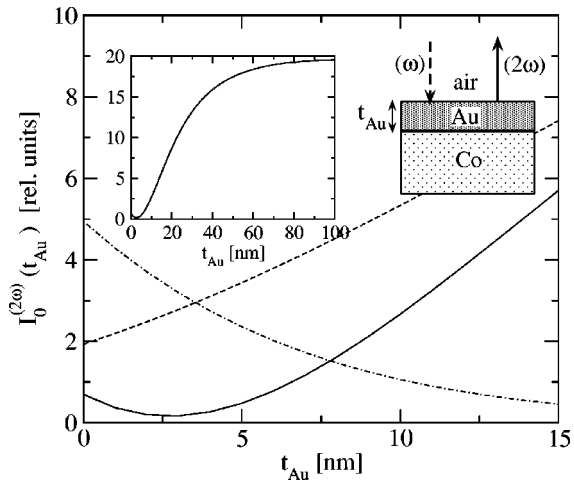

FIG. 5. The dependence of the SH intensity $I_0^{(2\omega)}$ on the thickness of the Au layer. The SH field is observed in air at the angle $\theta_0^{(2\omega)}=0°$. The dashed and dash-dotted lines correspond to the contributions originating from the top air/Au interface and the buried Au/Co interface, respectively. The total SH intensity, given by the combination of these two contributions, is depicted by the solid line. The structure under consideration is shown in the graph inset. The graph in the inset shows the total SH intensity variation over an extended range of thickness of the Au layer.

It is clear from the above account that the calculation of a result involves a rather large number of steps. In order to facilitate the calculation, we designed a computer program that implements these steps. The results are presented below.

A. SH intensity as a function of layer thickness

In this example we consider a structure consisting of a thin Au layer deposited on a Co substrate. We show that when equivalent parameters describing the structure are used, the same results as those reported by Wierenga *et al.*[1] are obtained.

The cross section of the structure is depicted in the inset of the graph in Fig. 5. The structure is illuminated by a fundamental beam ($\lambda^{(\omega)}=532$ nm) from air at the incident angle of $\theta_0^{(\omega)}=0°$. The magnetization is considered to be zero. The optical parameters of the materials involved are taken from the literature.[41]

The symmetry analysis of the top air/Au (1) and buried Au/Co (2) interfaces implies that there are several nonzero elements of the tensors $\chi_{ijk,1}$ and $\chi_{ijk,2}$. However, for the purpose of this example, most of the elements are considered to be zero. The values of the non-zero elements are[1] $\chi_{yyy,2}=1$ and $\chi_{yyy,3}=-1.6$, and they are considered to be independent of the lateral coordinate y. This means, as discussed in Sec. II H, that the SH field is generated in such a direction that Eq. (92) is satisfied. In this case it means that the SH field can be observed either in air at $\theta_0^{(2\omega)}=0°$ or in the Co substrate at $\theta_2^{(2\omega)}=0°$. As the observation of the SH field radiated into the Co substrate is almost impossible, we analyze only the field radiated into the air superstrate.

Figure 5 shows the SH intensity observed in air as a function of the Au layer thickness, as calculated from Eq. (99). Due to the normal incidence and no magnetization involved, the **s** and **p** polarizations are interchangeable and thus do not need to be considered separately.

The contribution of the air/Au interface (depicted by a dashed line) is increasing with the thickness of the Au layer. This is mainly due to the fact that the amplitude of the fundamental field at this interface increases with the Au layer thickness. This is in contrast to the contribution of the Au/Co interface (depicted by a dash-dotted line) from which the contribution decreases with increasing thickness of the Au layer. This is again given by the rapid decrease of the fundamental field at this interface for thicker Au layers due to its strong attenuation within the Au layer.

The solid line shows the variation of the total SH intensity. It firstly decreases and reaches a minimum at a Au layer thickness of about 2.5nm, and then monotonically increases until it saturates (see the graph inset). As can be seen, the minimum intensity is reached at a thickness for which the separate contributions from each interface are relatively high. This is due to destructive interference effects taking place when the two contributions are considered together. In other words, even though the contributions from each interface are relatively large, if their phases are opposite they can cancel each other out.

B. MSHG intensity as a function of incident angle

In this example, we consider a structure consisting of a Au(3nm)/Co(3nm)/Au(25nm) trilayer deposited on a glass substrate and covered by air. This structure was experimentally studied in the literature.[8,9,31]

The fundamental **p**-polarized beam ($\lambda^{(\omega)}=632.8$nm) interrogates the structure from the glass substrate. The plane given by the beam propagation and its polarization vector is parallel to the *y*-*z* plane. The SH field is observed in the glass substrate in the same plane. The optical parameters of the materials involved are taken from the literature.[41]

The Co layer is assumed to be homogeneously magnetized in the transversal direction, i.e., $\mathcal{M}||\hat{x}$. The nonlinear properties of the air/Au, Au/Co, Co/Au, and Au/glass interfaces are described by the susceptibility tensors $\chi_{ijk,1}$, $\chi_{ijk,2}$, $\chi_{ijk,3}$, and $\chi_{ijk,4}$, respectively. Due to symmetry reasons, the susceptibility tensors of the top (2) and bottom (3) Au/Co interfaces are related by $\chi_{ijk,2}=-\chi_{ijk,3}$.

Similarly as in Sec. III A, most of the elements of the susceptibility tensors are assumed to be zero. The nonzero elements considered in the calculations are summarized in Table I. As follows from the symmetry arguments,[12,13] the elements $\chi_{zyy,1}$, $\chi_{zyy,2}=-\chi_{zyy,3}$, $\chi_{zyy,4}$ are nonmagnetic, while the elements $\chi_{yyy,2}=-\chi_{yyy,3}$ change sign upon a reversal of the magnetization of the Co layer.

The fundamental field impinges the multilayer system at an angle $\theta_4^{(\omega)}$. We assume that the values listed in Table I are constant along the corresponding interfaces, i.e., independent of on, *y*. Consequently, the SH field can be observed only in such a direction that Eq. (92) is satisfied, as discussed in Sec. II H. This means that for a fundamental beam incident at a particular angle $\theta_4^{(\omega)}$, there exists two SH beams, one propagating in the glass substrate at $\theta_4^{(2\omega)}$ and the other in the air superstrate at $\theta_0^{(2\omega)}$. These angles are related by Eqs. (92), (76), and (36). Below, only the SH beam radiated into the glass substrate is discussed.

TABLE I. Values of the elements of the susceptibility tensors considered in the calculations in Sec. III B. The values are given for two orientations of the Co layer magnetization. Elements which are not listed are identically zero.

$\mathcal{M}$	$\chi_{zyy,1}$	$\chi_{yyy,2}=-\chi_{yyy,3}$	$\chi_{zyy,2}=-\chi_{zyy,3}$	$\chi_{zyy,4}$
[1,0,0]	1	1	−2	−1
[−1,0,0]	1	−1	−2	−1

The form of the susceptibility tensors implies that the SH field generated by the trilayer structure is **p** polarized. When the SH intensity is evaluated for various incident angles $\theta_4^{(\omega)}$ of the fundamental field, the angular distribution looks as shown in Fig. 6. The figure also shows the corresponding magnetic contrast, which is calculated from Eq. (102).

The variation of the SH intensity with $\theta_4^{(2\omega)}$ is determined mainly by the dependence of the fundamental field at each interface on the incident angle $\theta_4^{(\omega)}$. That is, if the *y* component of the fundamental electric field was evaluated,[42] its variation with the incident angle $\theta_4^{(\omega)}$ would look very similar to that depicted in Fig. 6.

The angular range, for which the SH intensity is plotted, corresponds to the range of angles for which the surface plasmon is excited by the fundamental field. This phenom-

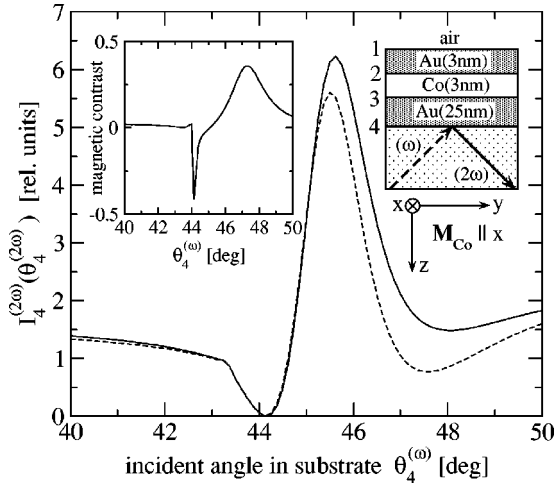

FIG. 6. Variation of the intensity of the SH **p**-polarized field with the incident angle $\theta_4^{(\omega)}$ of the **p**-polarized fundamental field. The SH beam is observed at an angle $\theta_4^{(2\omega)}$ which is related to $\theta_4^{(\omega)}$ via Eqs. (92), (76), and (36). The dependence was calculated for a trilayer system which is depicted in the graph inset and whose parameters are listed in Table I. The solid and dashed lines correspond to the magnetization of the Co layer in the $+\hat{x}$ and $-\hat{x}$ directions, respectively. The angular dependence of the magnetic contrast defined in Eq. (102) is plotted in the graph inset.

enon is accompanied by enhancement of the magnitude of the fundamental field at each interface at or around a particular incident angle. This is in close correlation with the observed enhancement of the SH intensity at the corresponding observation angle $\theta_4^{(2\omega)} \approx 45.5°$. These results agree with the experimental observations reported in the literature.[8,9,31]

C. Angular distribution of SH intensity from a layer with magnetic domains

In the previous two examples, we demonstrated the capabilities of the model on structures that have already been dealt with previously. The obtained results were found to be in agreement with those published in the literature.[1,8,9,31] In this section, we show that the capabilities of our model go beyond those discussed above. This is mainly due to the model's convenient formalism which culminates in Eqs. (85) and (88).

As a model structure, we consider the same trilayer system as in Sec. III B; however, in this case the Co layer contains magnetic domains. The domains are assumed to be separated by infinitely thin domain walls parallel to the *x*-*z* plane. The magnetization of the domains is changing periodically between the saturated values $\mathcal{M}^{\uparrow} \equiv [1,0,0]$ and $\mathcal{M}^{\downarrow} \equiv [-1,0,0]$ with a periodicity Δ, as shown in Fig. 7(a). In this example, we also consider the same values of the susceptibility tensor elements as in Sec. III B, which are summarized in Table I.

A phenomenological treatment of the SHG originating from a thin magnetic film containing periodic magnetic domain structures was already reported in the literature.[43–45] It was found that, in addition to the interface contributions, the SH field can also originate from the magnetic walls due to a nonzero value of the magnetization gradient $\nabla \mathcal{M}$ in this region. This follows from the fact that the expansion of the magnetically active susceptibility tensor χ_{ijk} in the magnetization contains terms proportional to $\nabla \mathcal{M}$. As a consequence of the periodicity of the domain structure, the generated SH field was found to exhibit a ''diffractionlike'' pattern, i.e., the illumination of the structure with a single fundamental beam could result in a diffraction pattern of the SH beams.

The model developed in Sec. II neglects the contributions to the SH field originating from locations other than those at the layer interfaces, such as those from the magnetic domain walls located in the layer bulk. Although it would be, in principle, possible to take such contributions into account by expanding the region of the integration of the point dipole contributions to more than just one (*y*) dimension [see Eq. (83)], it would go beyond the scope of this paper, and thus will not be treated here. Instead, the possible contributions originating from the domain walls will be neglected.

As can be seen from Table I, the elements $\chi_{yyy,2}$ and $\chi_{yyy,3}$, which correspond to the top and bottom Au/Co interfaces, respectively, are the only ''magnetically active'' components of the susceptibility tensors involved in the calculation. Assuming that the variation of the magnetization at these two Au/Co interfaces is the same as that of the Co layer

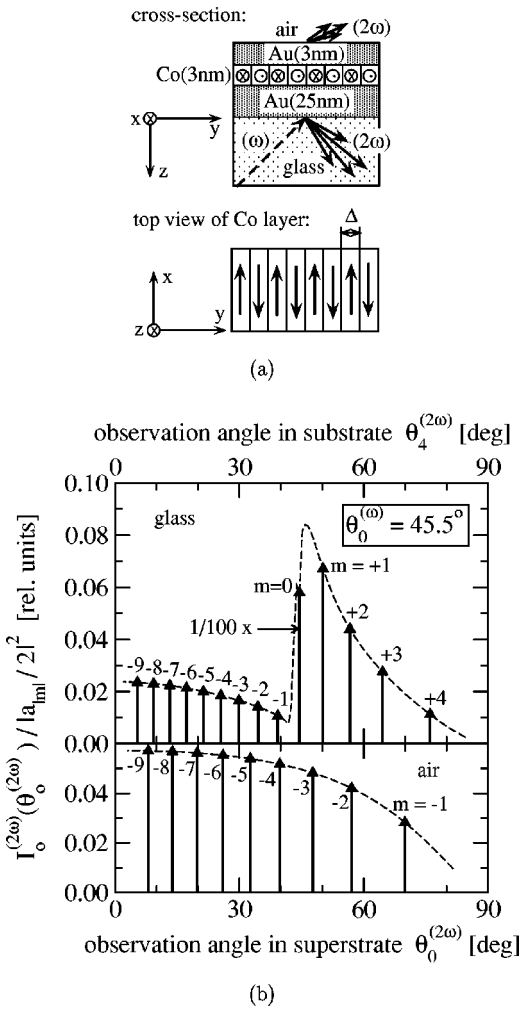

FIG. 7. (a) A cross section and a top view of the structure consisting of a Au/Co/Au trilayer deposited on a glass substrate. The magnetization of the Co layer varies periodically along the *y* coordinate with periodicity Δ. (b) The angular distribution of the SH intensity (**p**-polarized light) generated by a **p**-polarized fundamental beam. The fundamental beam illuminates the structure from glass at an incident angle of $\theta_4^{(\omega)} = 45.5°$. The normalized intensities, i.e., $I_0^{(2\omega)}(\theta^{(2\omega)})/|a_{|m|}/2|^2$, observed at discrete angular positions are depicted by the solid-line spikes ended with the up triangles. The numbers $m = 0, \pm 1, \pm 2, \ldots$ refer to the diffraction orders. The SH beams observed in the glass substrate and the air superstrate are plotted in the top and bottom graphs, respectively. The dashed line depicts the envelope of the angular distribution of the normalized intensities.

described above, the magnetically active tensor elements are described by a periodic function

$$\chi_{yyy,2}(y) = -\chi_{yyy,3}(y) = \begin{cases} 1 & \text{for } y \in \langle -\frac{1}{4}\Delta + n\Delta, \frac{1}{4}\Delta + n\Delta \rangle \\ -1 & \text{for } y \in (\frac{1}{4}\Delta + n\Delta, \frac{3}{4}\Delta + n\Delta), \end{cases} \tag{103}$$

where $n = 0, \pm 1, \pm 2, \ldots$. This function can be expressed in the Fourier series as

$$\chi_{yyy,2}(y) = -\chi_{yyy,3}(y) = \sum_{m=1}^{\infty} a_m \cos\left(m\frac{2\pi}{\Delta}y\right),$$

$$a_m = \frac{4}{\pi}\frac{(-1)^{m+1}}{2m-1}. \quad (104)$$

Consequently, the Fourier transform (87) takes the form

$$\mathcal{FT}[\chi_{yyy,2}](u) = -\mathcal{FT}[\chi_{yyy,3}](u) = \sum_{m=-\infty}^{\infty} \frac{a_m}{2}\left[\delta\left(u - m\frac{2\pi}{\Delta}\right)\right], \quad a_0 \equiv 0. \quad (105)$$

As shown in Table I, the tensor elements $\chi_{zyy,1}$, $\chi_{zyy,2} = -\chi_{zyy,3}$ and $\chi_{zyy,4}$ are magnetically inactive. This means that even though the magnetization of the Co layer varies along the y coordinate, these values remain independent of y. Consequently, their Fourier transforms are expressed as

$$\mathcal{FT}[\chi_{zyy,\nu}](u) = \chi_{zyy,\nu}(0)\,\delta(u), \quad \nu = 1,2,3,4. \quad (106)$$

When results (105) and (106) are substituted into Eqs. (88)–(91), the far-field SH intensity is found to be comprised of two contributions. The first contribution originates from the nonmagnetic part of the susceptibility tensors and is non-zero at such an angle that the equation

$$N_y^{(2\omega)} = N_y^{(\omega)} \quad (107)$$

is fulfilled. The second contribution to the SH intensity originates from the magnetic part of the susceptibility tensors. Equation (105) implies that it is qualitatively different from the nonmagnetic contribution in such a way that the SH intensity is non-zero only at such angles that

$$N_{y,m}^{(2\omega)} = N_y^{(\omega)} + m\frac{K_\Delta}{k_0^{(2\omega)}}, \quad K_\Delta \equiv \frac{2\pi}{\Delta}, \quad m = \pm 1, \pm 2, \ldots \quad (108)$$

is satisfied. This means that, due to the presence of the magnetic domains, the angular profile of the SH intensity comprises a diffraction pattern of SH beams characterized by a diffraction order m. This is in a qualitative agreement with the results reported in the literature.[43–45]

Comparing Eqs. (107) and (108), the nonmagnetic contribution to the SH field can be thought of as a zero diffraction order of the SH diffraction pattern. Therefore, studying the zero order of the SH diffraction pattern can reveal information about the nonmagnetic part of the susceptibility tensors, while the higher diffraction orders contain the information about the magnetic part of the susceptibility tensors.

The electrical fields corresponding to the diffraction orders can be evaluated employing Eqs. (88)–(91). Using the point-dipole approach to the SH problem, this evaluation can be illustratively interpreted as follows. The fundamental field ''creates'' four *magnetically inactive point dipoles,* each placed at one of the interfaces at the positions characterized by equal values of y (such as $y=0$). These point dipoles radiate anisotropically into the surrounding media. The angular distribution of the electric field radiated by each dipole is given by Eq. (82). The SH far-field intensity corresponding to the zero diffraction order is subsequently obtained by summing up the field contributions of these four point dipoles and evaluating the intensity at such a value of the observation angle that Eq. (107) is satisfied.

A similar interpretation can be considered for the higher SH diffraction orders ($|m| \geqslant 1$). In this case, Eq. (105) implies that there are two *magnetically active point dipoles* ''created'' by the fundamental field. Both are located at position characterized by the same value of y as the four magnetically inactive dipoles mentioned above (such as $y=0$). The two magnetically active dipoles radiate anisotropically into the surrounding media with the angular distribution described by Eq. (82). The SH far-field intensity corresponding to the diffraction order m is subsequently obtained by summing up the field contributions of these two point dipoles and evaluating the intensity at such a value of the observation angle that Eq. (108) is satisfied. Moreover, the intensity at this angle has to be multiplied by the factor $|a_{|m|}/2|^2$, as follows from Eq. (105).

The results discussed above imply that by studying the diffraction pattern of the SH field, one can gather information about the domain structure of the buried magnetic interfaces, or even the layers themselves, provided that the relation between the layer and interface magnetization is known. This is feasible only if the experimental configuration guarantees that the conditions which justify the use of Eq. (87) for the evaluation of the quantity $\mathcal{FT}[\chi_{ijk,\nu}](u)$ are fulfilled. These conditions require that the magnitude of the fundamental field across the area illuminated by the fundamental beam is uniform, and that the width of this area is much greater than the domain periodicity Δ. If these conditions are not satisfied, Eq. (87) would have to be slightly modified to take into account not only the distribution of the phase of the fundamental field but also the profile of the field magnitude across the illuminated area. This would, however, go beyond the scope of this paper and therefore will not be dealt with in a greater detail.

To visualize the results discussed above, we plot the angular distribution of the SH intensity generated by a **p**-polarized fundamental beam ($\lambda^{(\omega)} = 632.8$nm) illuminating the structure from the glass substrate at an incident angle of $\theta_4^{(\omega)} = 45.5°$. The results, which were calculated for $\Delta = 10\lambda^{(2\omega)} \approx 3.2$ μm, are shown in Fig. 7(b). The spikes ending with the up triangles represent the angular positions of the diffracted SH beams, each characterized by the diffraction order m.

In order to make the graphical representation clearer, the values of the SH intensities, which are represented by the spikes length, are multiplied by the corresponding factors $|a_{|m|}/2|^{-2}$ for $|m| \geqslant 1$. Furthermore, to enable the visualization of the zero diffraction order in the same scale as the higher diffraction orders, its intensity was multiplied by a factor of 1/100. In the following discussion, the intensity values multiplied by the corresponding factor $|a_{|m|}/2|^{-2}$ for $|m| \geqslant 1$ will be referred to as the normalized SH intensities.

When the scales of the y axis of the graphs in Figs. 6 and 7 are compared, it can be seen that the normalized intensities of the higher diffraction orders are considerably smaller than that of the zero order. This difference is pronounced even more when the true values of the SH intensity, i.e., the normalized intensities multiplied by the corresponding factors

$|a_{|m|}/2|^2$, are considered. This difference in the magnitude of the SH intensity is solely due to the numerical values of the elements of the susceptibility tensors used in the calculation.

The dashed line in Fig. 7(b) represents the envelope of the angular profile of the normalized intensities of the diffracted SH beams. It is determined by the radiation of two magnetically active point dipoles placed at the top and bottom Au/Co interfaces, as explained above. This envelope is useful if one is interested in the modification of the diffraction pattern of the SH beams implied by the change of the domain periodicity Δ, while all the other parameters remain unmodified. In this case, the positions of the diffraction orders (spikes) would be shifted so as to fulfill Eq. (108), while the normalized intensities (lengths of the spikes) would follow the envelope which remains unchanged. The true values of the SH intensities are then evaluated by multiplying the normalized values by the corresponding factors $|a_{|m|}/2|^2$.

It is important to note that the envelope varies with the incident angle of the fundamental beam. This is due to the fact that the magnetically active elementary dipoles, which are generated by the fundamental field at the Au/Co interfaces, vary their magnitude[46] due to the dependence of the fundamental field itself on the incident angle. This implies that the normalized intensities of the diffracted SH beams corresponding to different diffraction orders vary with the incident angle of the fundamental beam. An example of this variation is shown in Fig. 8(a), where the envelopes depicted by the solid, dashed, and dash-dotted lines correspond to the incident angle of $\theta_4^{(\omega)}=45.5°$, 40°, and 50°, respectively. The graph demonstrates that the envelopes, and thus the normalized intensities of the diffracted SH beams, can vary substantially even for as small variations of the incident angle as $\pm 5°$.

Another interesting result follows from the analysis of the dependence of the SH intensity of a particular diffraction order on the incident or observation angle. The variation of the incident angle $\theta_4^{(\omega)}$ of the fundamental beam implies that the angles, at which the diffracted SH beams are observed, vary. This variation is described by Eq. (108) for the diffraction orders $|m|\geqslant 1$ and by Eq. (107) for the zero order. The corresponding variation of the SH intensity can be calculated as discussed above, i.e., using Eqs. (85)–(91).

Following these steps, the SH intensity of the diffraction orders $m=0,\pm 1$ was calculated as a function of the corresponding observation angles $\theta_4^{(2\omega)}$ in the glass substrate. The result is shown in Fig. 8(b). In the calculation, the incident angle of the fundamental field varies in the range of $\theta_4^{(\omega)}\in\langle 40°,50°\rangle$. Consequently, the SH beams of the orders $m=1$, 0, and -1 could be observed at angles $\theta_4^{(2\omega)}\in\langle 34.3°,43.3°\rangle$, $\theta_4^{(2\omega)}\in\langle 39.5°,48.8°\rangle$, and $\theta_4^{(2\omega)}\in\langle 44.7°,55.1°\rangle$, as depicted by the dashed, solid, and dash-dotted lines, respectively. In addition to the strong variation of the *magnitude* of the SH intensity between the different diffraction orders, it is also the angular profile that varies considerably between the diffraction orders. These differences are associated with the fact that the radiation of a point dipole itself exhibits strong angular anisotropy due to the interaction with the surrounding multilayer system, as discussed in the literature.[23,24,47] Due to this anisotropy, different orders of the diffracted SH beams, which propagate at different angles, exhibit different angular dependences of their corresponding intensity.

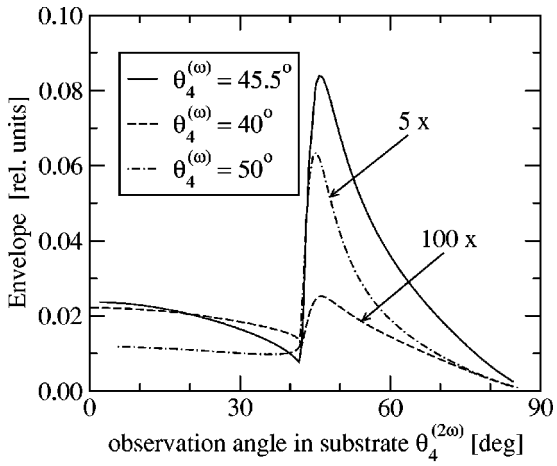

(a)

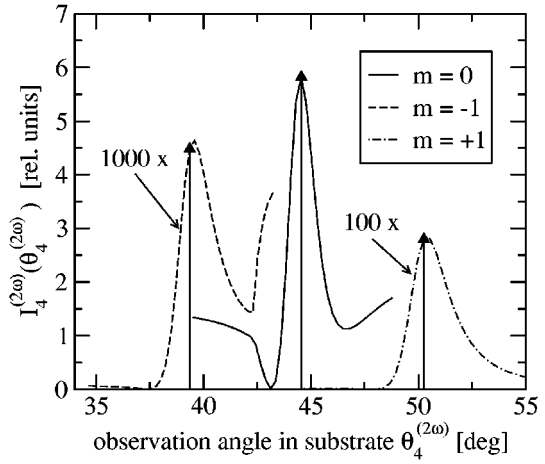

(b)

FIG. 8. (a) Envelopes of the SH diffraction patterns plotted for various values of the incident angle $\theta_4^{(\omega)}$ of the fundamental field; the solid, dashed and dash-dotted lines correspond to $\theta_4^{(\omega)}=45.5°$, 40° and 50°, respectively. The envelopes correspond to the SH diffraction patterns generated by the structure shown in Fig. 7(a). (b) The dependence of the SH intensity of the diffracted SH beam on its observation angle $\theta_4^{(2\omega)}$. The dependence plotted in the graph is a consequence of the variation of the incident angle $\theta_4^{(\omega)}$ of the fundamental beam in the range of $\theta_4^{(\omega)}\in\langle 40°,50°\rangle$. The solid, dashed, and dash-dotted lines correspond to the zero, first, and -1^{st}, diffraction orders, respectively. The spikes ending with the up triangles depict the angular positions and the corresponding intensities of the diffracted SH beams corresponding to $\theta_4^{(\omega)}=45.5°$.

IV. CONCLUSION

We developed a complete and comprehensive model and its computer implementation which is suitable for a description and evaluation of the second-harmonic generation (SHG) from arbitrary multilayer systems. The model was

developed under the following fundamental assumptions.

(i) The multilayer structure is assumed to consist of arbitrary homogenous materials, including lossy, anisotropic and magneto-optic media. Optical properties of each layer (complex permittivity tensor, thickness) are assumed to be constant in the lateral dimension.

(ii) The second-harmonic field is generated by a set of electric point dipoles located at the interfaces of the multilayer structure, as a result of the local symmetry breaking. The complex amplitude of the dipoles is evaluated using a phenomenological description of the surface nonlinearity, i.e., by multiplying the square of the fundamental field with the susceptibility tensor assigned to each interface.

(iii) The total second-harmonic response of the multilayer structure is calculated by the summation of all the single-dipole contributions over the entire multilayer structure. In this process, an arbitrary spatial distribution of the susceptibility tensor can be accounted for.

The point dipole approach proves to be very convenient and powerful, both from the formal and computational points of view. It can be applied in almost any situation (employing planar geometry) where the spatial distribution of the source of the SH field is known or to be studied. Due to the convenient matrix formalism used, the treatment is also very compact, elegant and can be easily implemented into a computer program.

The model was applied in the area of magnetic-induced second-harmonic generation (MSHG), where the SHG experiments provide a useful tool for studying the magnetic properties of interfaces. The model was used to study the dependence of the SH intensity on the thickness of one of the layers and on the incident angle of the fundamental beam. The systems under consideration employed interfaces with constant values of the nonlinear susceptibility tensors. The obtained results were found to be in a complete agreement with those published in the literature.

The elegance of the developed model becomes apparent when the systems with an unhomogeneous distribution of the susceptibility tensors along the interfaces are considered. This can happen, for example, in the area of MSHG, where the magnetization of the layers, and thus the interfaces, exhibits variations in the lateral dimension due to, for example, the presence of magnetic domains, propagating spin waves, magnetic nanostructures, etc., and where the optical properties (layer thicknesses and permittivity tensors) can be assumed to be laterally homogeneous. To demonstrate the capabilities of the model, we considered a trilayer system in which one of the layers contained magnetic domains with periodically changing orientations. We found that the single beam of the SH field, which corresponds to the situation with a uniformly distributed magnetization, is transformed into a ''diffraction pattern'' of the SH beams with the angular spacing related to the domain periodicity. In addition to the angular spacing of the diffracted SH beams, the model is also able to predict the intensity of a particular diffraction order and its relation to the parameters characterizing the nonlinear properties of the interface. Because the SH field can, in principle, be generated from any buried interface, the model can be used as the grounds for the analysis of the magnetic domains or other magnetic inhomogeneities of buried layers.

This is one of many possible implications that can be derived using the formalism developed in this work. The number of parameters involved in the calculations is vast, which can make the experimental realization of the implications somewhat problematic. Nevertheless, the point dipole approach and its conveniently formalized implementation have a good potential for designing and analyzing the experiments in the area of MSHG or in any other area where the second-harmonic generation from multilayer systems is of interest.

Although the theory presented in this paper was developed while considering several restrictions, the convenient and compact formalism penetrating the work allows for its rather straightforward expansion. The restriction to a one-dimensional variation of the nonlinear susceptibility tensors can easily be removed by expanding the description of the fundamental and SH fields to three dimensions $(x-y-z)$, as opposed to the two-dimensional description $(y-z)$ presented here. The model also considers that the point dipoles generated by the fundamental field radiate coherently. Due to the point-dipole nature of the model, this could also be expanded to situations where some mechanism decorrelates, either spatially or in the time domain, the dipole radiation. Finally, the model could be expanded so as to describe nonlinear systems with *arbitrarily spatially distributed* sources of the SH field, as opposed to the hereby analyzed systems in which the SH field originates solely from the layer interfaces.

ACKNOWLEDGMENTS

The authors (J.H. and L.P.) would like to thank the Laboratoire de Physique des Solides at the Université Paris-Sud in Orsay, France, for their hospitality and for providing a fruitful working atmosphere. Professor Š. Višňovský is gratefully acknowledged for his advice and permanent encouragement for this work. This research was supported through the EuropeanCommunity Marie Curie Fellowship Contract No. HPMT-CT-2000-00066 (L.P.) and benefitted from the grant of the French Ministère des affaires étrangères (J.H.). This work has been supported by the Grant Agency of the Czech Republic No. 202/03/0776.

*Corresponding author. Email address: hamrle@karlov.mff.cuni.cz

[1] H.A. Wierenga, M.W.J. Prins, and T. Rasing, Physica B **204**, 281 (1995).

[2] K.H. Bennemann, J. Magn. Magn. Mater. **200**, 679 (1999).

[3] U. Conrad, J. Güdde, V. Jähnke, and E. Matthias, Phys. Rev. B **63**, 144417 (2001).

[4] P. Guyot-Sionnest, W. Chen, and Y.R. Shen, Phys. Rev. B **33**, 8254 (1986).

[5] A. Kirilyuk, T. Rasing, M.A.M. Haast, and J.C. Lodder, Appl. Phys. Lett. **72**, 2331 (1998).

[6] B. Koopmans, A.M. Janner, H.A. Wierenga, T. Rasing, G.A. Sawatzky, and F. van der Woude, Appl. Phys. A: Mater. Sci. Process. **60**, 103 (1995).

[7] V.A. Kosobukin, J. Magn. Magn. Mater. **153**, 397 (1996).

[8] V.V. Pavlov, G. Tessier, C. Malouin, P. Georges, A. Brun, D. Renard, P. Meyer, J. Ferré, and P. Beauvillain, Appl. Phys. Lett. **75**, 190 (1999).
[9] G. Tessier, C. Malouin, P. Georges, A. Brun, D. Renard, V.V. Pavlov, P. Meyer, J. Ferré, and P. Beauvillain, Appl. Phys. B: Lasers Opt. **68**, 545 (1999).
[10] H.A. Wierenga, W. de Jong, M.W.J. Prins, T. Rasing, R. Vollmer, A. Kirilyuk, H. Schwabe, and J. Kirschner, Phys. Rev. Lett. **74**, 1462 (1995).
[11] V.L. Brudny, W.L. Mochán, B.S. Mendoza, A.V. Petukhov, and T. Rasing, IEEE Trans. Magn. **34**, 1048 (1998).
[12] R.-P. Pan, H.D. Wei, and Y.R. Shen, Phys. Rev. B **39**, 1229 (1989).
[13] R. Birss, in *Symmetry and Magnetism*, edited by E. P. Wohlfarth (North-Holland, Amsterdam, 1964).
[14] The phrases ''everywhere'' and ''almost everywhere'' need to be understood in the sense of the measure theory.
[15] We recall that the media comprising the multilayer structure are considered to be magnetically inactive (i.e., $\mu^{(\omega_0)} \equiv \mu_0$), as mentioned in Sec. II B.
[16] C. Chappert, H. Bernas, J. Ferré, V. Kottler, J.P. Jamet, Y. Chen, E. Cambril, T. Devolder, F. Rousseaux, V. Mathet, and H. Launois, Science **280**, 1919 (1998).
[17] T. Aign, P. Meyer, S. Lemerle, J. Jamet, J. Ferré, V. Mathet, C. Chappert, J. Gierak, C. Vieu, F. Rousseaux, H. Launois, and H. Bernas, Phys. Rev. Lett. **81**, 5656 (1998).
[18] P. Warin, R. Hyndman, J. Glerak, J. Chapman, J. Ferré, J. Jamet, V. Mathet, and C. Chappert, J. Appl. Phys. **90**, 3850 (2001).
[19] S. Landis, B. Rodmacq, B. Dieny, B. Dalzotto, S. Tedesco, and M. Heitzmann, J. Magn. Magn. Mater. **226–230**, 1708 (2001).
[20] In the following analysis, most of the expressions for the magnetic field are similar to those for the electric field and will not therefore be written explicitly.
[21] M. Born and E. Wolf, *Principles of Optics* (Pergamon, Oxford, 1959).
[22] L. Landau and E. Lifschitz, *Electrodynamics of Continuous Media* (Pergamon Press, Oxford, 1960).
[23] G.W. Ford and W.H. Weber, Phys. Rep. **113**, 195 (1984).
[24] L. Polerecky, J. Hamrle, and B.D. MacCraith, Appl. Opt. **39**, 3968 (2000).
[25] Again, an isotropic medium (ϵ_ν) is considered.
[26] P. Yeh, Surf. Sci. **96**, 625 (1980).
[27] S. Visnovsky, Czech. J. Phys., Sect. B **36**, 625 (1986).
[28] K. Ohta and H. Ishida, Appl. Opt. **29**, 1952 (1990).
[29] L. Mandel and E. Wolf, *Optical Coherence and Quantum Optics* (Cambridge University Press, Cambridge, 1995).
[30] P. Yeh, *Optical Waves in Layered Media* (Wiley, New York, 1988).
[31] G. Tessier, Ph.D. thesis, Université de Paris-Sud U.F.R. Scientifique d'Orsay, 1999.
[32] T.F. Heinz, H.W.K. Tom, and Y.R. Shen, Phys. Rev. A **28**, 1883 (1983).
[33] A. Kirilyuk, J. Phys. D **35**, R189 (2002).
[34] R. Atkinson and N.F. Kubrakov, Phys. Rev. B **65**, 014432 (2001).
[35] F.W. Byron, Jr. and R. W. Fuller, *Mathematics of Classical and Quantum Physics* (Dover, New York, 1992).
[36] Note that the subscript z refers to the z component of the vector $\overline{\boldsymbol{D}}$.
[37] The equations expressing the boundary conditions were ordered in a way which is more suitable for further derivations.
[38] For simplicity, the explicit dependence on $N_y^{(\omega)}$ and $N_y^{(2\omega)}$ is omitted in this equation.
[39] The Fourier transform of a function f is denoted by $\mathcal{FT}[f](u)$, where u is the variable in the Fourier space.
[40] W. P. Schleich, *Quantum Optics in Phase Space* (Wiley–VCH, Berlin, 2001).
[41] E. D. Palik, in *Handbook of Optical Constants*, edited by E. D. Palik (Academic Press, London, 1985).
[42] The form of the susceptibility tensors considered in this calculation implies that the dipoles are generated only by the y component of the fundamental electric field.
[43] I.L. Lyubchanskii, J. Magn. Magn. Mater. **157/158**, 307 (1996).
[44] I.L. Lyubchanskii, A.V. Petukhov, and T. Rasing, J. Appl. Phys. **81**, 5668 (1997).
[45] N.N. Dadoenkova, I.L. Lyubchanskii, M.I. Lyubchanskii, and T. Rasing, Appl. Phys. Lett. **74**, 1880 (1999).
[46] The magnetically active dipoles can also vary their orientation, in particular if more magnetically active elements of the susceptibility tensors are considered to be non-zero.
[47] J. Enderlein, T. Ruckstuhl, and S. Seeger, Appl. Opt. **38**, 724 (1999).